This is to certify that the
thesis entitled

A Method for Modeling the Electrical Variable Transmission

presented by

Stephen M. Bohan

has been accepted towards fulfillment
of the requirements for the

M.S. degree in Electrical and Computer Engineering

EG Strangas
Major Professor's Signature

9 May 2008
Date

A Method for Modeling the Electrical Variable Transmission

By

Stephen M. Bohan

A THESIS

Submitted to
Michigan State University
in partial fulfillment of the requirements
for the degree of

MASTER OF SCIENCE

Department of Electrical and Computer Engineering

2008

ABSTRACT

A Method for Modeling the Electrical Variable Transmission

By

Stephen M. Bohan

The increasing price of fuel and concern for the environment has lead to the proliferation of hybrid electric vehicles. This has lead to the introduction of many new electric machines to try to create the maximum efficiency for the hybrid vehicle. In this thesis one such machine, the electric variable transmission, will be investigated. A model will be developed for the electric variable transmission and that model will be evaluated against a set of expected results to display its accuracy.

To my wife, Sarah

ACKNOWLEDGMENTS

I would first like to show my appreciation to Dr. Elias Strangas, my thesis advisor, for his guidance, patience, and support throughout this process. His technical expertise and experience gave me the tools needed to complete this work and to guide me in future endeavors. I also owe my gratitude to Dr. Gregory Wierzba and Dr. Guoming Zhu for giving their time and energy to be a part of my committee.

This work would not have been completed without the help of the people at my employer, BorgWarner, especially, my supervisors Mike Tuttle and Al Dove. I would also like to express my appreciation to my coworkers for understanding my odd hours and drowsiness during this process.

A special thank you is owed to all of my lab colleagues especially, Sinisa Jurkovic, Carlos Niño, and Wes Zanardelli.

Lastly and most importantly, I would like to express my deepest gratitude to my wife, Sarah. Without her love, support and understanding, none of this work would have been possible. It is to her that I dedicate this work.

TABLE OF CONTENTS

LIST OF TABLES

LIST OF FIGURES

CHAPTER 1

Introduction

High fuel costs and concern for the environment have led many vehicle manufacturers to introduce hybrid electric vehicles. In fact, Honda and Toyota have projected that 10% to 15% of the U.S. auto market will consist of hybrid electric vehicles by the year 2009[6]. Traditionally, hybrid electric vehicles have fallen into two categories: series and parallel. Recently, two new classifications have been added. Series-parallel and complex hybrids have been introduced to improve performance[2].

In a series hybrid, power is generated by an internal combustion engine which is connected to a generator. The generator powers a DC bus which is used to feed power to an electric motor. The electric motor then provides power to the wheels. A large benefit of a series hybrid is that the electric motor can also be used for regenerative braking to supply power back to the DC bus. Therefore, less power is lost due to braking. One major drawback of a series hybrid is that all of the power is transmitted through the electric components. Therefore, the electric components must be sized for worst-case power draw. This results in large motors, generators, and power electronics which can be very expensive and very heavy.

In a parallel hybrid, power can be delivered to the wheels either through an electric motor or directly from the internal combustion engine. As in a series hybrid, the motor can act as a generator during braking to reclaim power lost due to braking.

A parallel hybrid has an advantage over the series hybrid because it only requires one electric machine, the electric motor. This results in fewer component costs and weight which can hurt overall fuel economy. Another advantage is that all of the power does not need to be transmitted through the electrical system. This results in smaller power electronics and a smaller motor. Which will further add to the cost and weight benefit over the series hybrid.

The disadvantage of a parallel hybrid in comparison to the series hybrid is that the least efficient part of a hybrid vehicle system is usually the internal combustion engine. In a series hybrid, all of the power from the internal combustion engine must go through the electrical system. Therefore, the internal combustion engine can be operated at peak efficiency for the majority of its duty cycle. This is not the case for the parallel hybrid as the electrical system only provides a portion of the necessary power.

It would be best to get the efficiency benefits of operating an internal combustion engine at its peak efficiency as in the series hybrid but also benefit from the direct mechanical power transmission of the parallel hybrid. This is where series-parallel and complex hybrid systems come into play. To achieve this benefit, a machine must transmit some of its power directly and some of it through power electronics. There have been many proposals for a system which can do just that [1] [8].

This thesis will concentrate on one concept to meet this goal. Hoeijmakers and Ferreira introduced a new electrical machine, the Electrical Variable Transmission, (EVT)[4] which transmits power from the engine through both power electronics and directly through a magnetic coupling to the drive shaft. The EVT is essentially two concentrically arranged induction motors with a shared rotor. The shared rotor is constructed thinner than what the combination of the two rotors would be and therefore, introduces complexity into the machine. This complexity will be detailed later in this paper.

In this thesis, a model will be developed for the electric variable transmission. The concept of the EVT will be developed and evaluated. A method for finding the machine parameters will be introduced and implemented using finite elements analysis. The EVT model will then be developed. The model will be evaluated against a set of expected results to display its accuracy. The model will be investigated without operating with closed loop control. Control of the EVT is beyond the scope of this thesis but, it is an opportunity for future work.

CHAPTER 2

Electric Variable Transmission

2.1 Introduction to the EVT

To help understand how the EVT works, a simple case will first be investigated and complexity will be added to develop the concept.

2.2 The Cascade System

The system can first be thought of as two independent electrical machines with no electric port. It will be comprised of a conventional motor and a specialized generator linked only by a DC bus as seen in Figure 2.1. Electrical power from the first machine is withdrawn from brushes on its rotor. The brushed rotor of this machine acts similarly to how a stator would function in a traditional induction machine. The exterior rotor acts as a rotor in a traditional induction machine.

Power enters this system as mechanical power applied to the input shaft of the first machine

$$P_{m1} = \omega_{m1} T_{m1} \tag{2.1}$$

where ω_{m1} is the rotational speed and T_{m1} is the mechanical torque. For simplicity, it is assumed that this system is lossless. After entering the system as mechanical

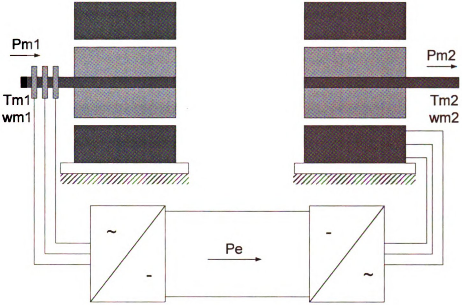

Figure 2.1. Cascaded Dual Machine System

power, the power is then converted to electrical power, P_e, by the first machine and fed through a rectifier to create a DC voltage. This DC voltage is fed through an inverter, which supplies electrical power to the second machine. This electrical power is converted back to mechanical power, P_{m2}, by the second machine providing power on the shaft of the second machine.

$$P_{m2} = \omega_{m2} T_{m2} \tag{2.2}$$

If this system is not lossless, as it is in reality, the numerous power conversions of this method result in relatively low efficiency.

2.3 The Dual Linked System

The efficiency of the cascaded system could be greatly increased by directly transmitting a portion of the input power to the shaft of the second machine. This could

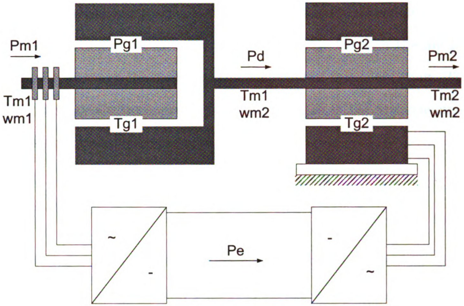

Figure 2.2. Dual Linked System

be done by connecting the outer rotor of the first machine to the rotor of the second machine, as seen in Figure 2.2.

If this new system is assumed to be lossless, the power transmitted through the airgap of the first machine, P_{g1}, can be thought of as a function of two components. The first component is converted to electrical power, P_e, and is a function of both shaft speeds and the electromagnetic field torque, T_{g1}.The electromagnetic field torque of machine one will be equal to the input torque.

$$P_e = (\omega_{m1} - \omega_{m2})T_{g1} = (\omega_{m1} - \omega_{m2})T_{m1} \tag{2.3}$$

The electrical power is transmitted through the rectifier and inverter and then through the air gap of the second machine, P_{g2}, as it was in the cascaded system.

$$P_{g2} = P_e \tag{2.4}$$

The electrical power only accounts for part of the power transmitted to the second machine. The rest of the power is transmitted directly through the air gap of the first machine, P_d, through the mechanical linkage to the secondary shaft. This power is due to the primary electromagnetic torque in the gap of the first machine and the speed of the linked rotors.

$$P_d = \omega_{m2} T_{g1} = \omega_{m2} T_{m1} \tag{2.5}$$

The power transmitted through the system could be represented by summing the electrical power and the power that is directly transmitted.

$$P_{m1} = P_e + P_d = P_{m2} \tag{2.6}$$

As was the case with the cascade system, some power is transmitted through the electrical components, P_e, with relatively high losses. But now, a portion of the power is also transmitted directly to the second machine, $P_{g1} = P_d$, through the air gap of the first machine. This power can be assumed to have relatively low losses.

Figure 2.3 depicts a situation in which the input torque, T_{m1}, and speed, ω_{m1}, are held constant. Since direct power transmission is generally more efficient then electrical power transmission, efficiency will increase as ω_{m2} approaches ω_{m1}. The portion of the graph where ω_{m2} is low is intentionally not represented because the assumption of a lossless system is especially erroneous in this region.

Just as the power transmitted through the primary machine is comprised of two components, the output torque of the machine also consists of two components. One component, T_{g1}, is transmitted through the air gap of the first machine.

$$T_{g1} = T_{m1} \tag{2.7}$$

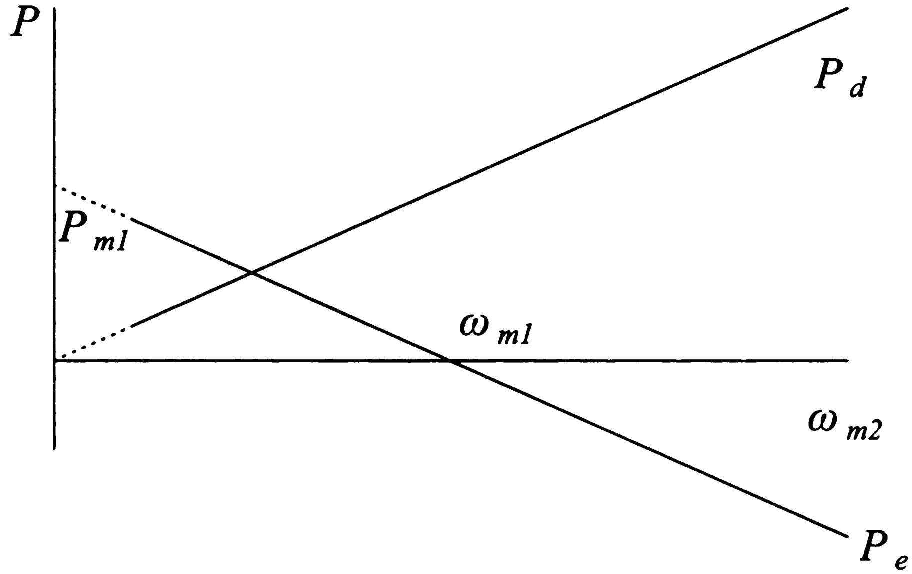

Figure 2.3. Power distribution with respect to speed under constant torque

The other component, T_{g2}, is transmitted through the air gap of the secondary machine and is a result of the electric power transmitted through the system.

$$T_{g2} = \frac{P_e}{\omega_{m2}} = \frac{\omega_{m1} - \omega_{m2}}{\omega_{m2}} T_{m1} \tag{2.8}$$

Equations (2.7) and (2.8) can be combined to show the relationship between the input and output torque.

$$T_{m2} = \frac{\omega_{m1}}{\omega_{m2}} T_{m1} \tag{2.9}$$

As it was in equation (2.9) $T_{m2} = T_{m1}$ when $\omega_{m2} = \omega_{m1}$. At this point, all torque is transmitted through T_{g1} resulting in the most efficient torque transmission. When the input speed is equal to the output speed, all of the power, and subsequently torque, will be transmitted directly as P_d. This implies that all torque will be transmitted directly through T_{g1} and no torque will be transmitted though T_{g2}. This should lead to the highest efficiency as all of the power is transmitted through the path with the fewest components.

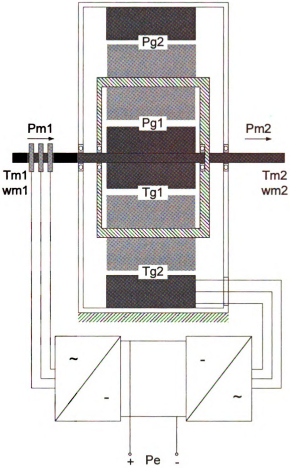

Figure 2.4. Concentric implementation of the dual linked system

2.4 Concentric Implementation

In order to save space in the implementation of the dual linked system, the two machines could be arranged concentrically where the mechanically linked rotor is now a shared rotor with two sets of windings as seen in Figure 2.4. Since the stator of the first machine is not stationary it will be referred to as the inner rotor. Consequentially, the shared rotor of the two machines will be referred to as the outer rotor.

So far, losses have been ignored except after the power flow has been developed. In reality some key power losses should be considered while developing the power flow through the machine. The power equations for this machine will be derived taking into account key power losses.

The system is supplied by the shaft power of machine 1, $P_{m1} = \omega_{m1} T_{m1}$. It is then split into two separate parts. The first part is transmitted directly to the shared rotor through the first air gap

$$P_{dg1} = \omega_{g1} T_{g1} \tag{2.10}$$

where ω_{g1} is the rotational speed of the field in the inner air gap. The rotational speed of the field in the air gap is supplied by the frequency of the inner rotor currents, ω_{ir1}, spinning at input speed, ω_{m1}, producing the following relationship.

$$\omega_{g1} = \omega_{ir1} + \omega_{m1} \tag{2.11}$$

As it was in the dual linked system, the torque in the gap is equal to the input torque, $T_{g1} = T_{m1}$. The rotor losses of the first machine will now be considered. In an induction machine, the rotor losses are a function of the slip in the machine. In this case, the slip speed is the difference of the inner rotor frequency of machine 1, ω_{g1}, and the rotor speed of machine 1. For the concentric implementation, the rotor of machine 1 is mechanically linked to the rotor of machine 2. Since the mechanical speed of machine 2 is the outer rotor speed, the outer rotor speed is equal to the output speed, ω_{m2}

$$\omega_{or1} = p(\omega_{g1} - \omega_{m2}) \tag{2.12}$$

where p is the number of pole pairs in machine 1. The outer rotor power losses due to machine 1 can be estimated as

$$P_{or1,losses} = \frac{\omega_{or1}}{p} T_{m1} \tag{2.13}$$

The power transmitted directly, P_d, is then found by subtracting the losses from the power transmitted directly through the air gap

$$P_d = (\omega_{g1} - \frac{\omega_{or1}}{p})T_{m1} \tag{2.14}$$

The remaining power flowing through the first machine is transmitted as electrical power. As was the case with the direct power transfer, the power transmitted through the inverter also suffers from machine losses. This time, the losses are first due to the inner rotor of machine 1, $P_{ir,losses}$. Since the inner rotor functions as a stator would in a traditional induction machine, the winding losses can be treated the same as they would be in a traditional stator. Stator winding losses are a function of machine parameters and are independent of frequencies. As such, they will not be derived. After removing inner rotor losses, the electrical power transmitted through the air gap of machine and into the inner rotor will then be

$$P_{ir} = P_e = (\omega_{m1} - \omega_{g1})T_{m1} - P_{ir,losses} \tag{2.15}$$

P_{ir} is supplied to the power electronics as P_e where it again suffers losses, $P_{e,losses}$. The power is transmitted next through the stator of the second machine with losses $P_{s,losses}$ and into the air gap between the second machine and the outer rotor

$$P_{g2} = P_e - P_{e,losses} - P_{s,losses} \tag{2.16}$$

P_{g2} can be related directly to the torque in the second air gap T_{g2}

$$P_{g2} = \omega_s T_{g2} \tag{2.17}$$

where, ω_s is the frequency of the currents in the stator.

Before it is finally transmitted as output power, it suffers one more set of losses from the outer rotor due to the second machine, $P_{or2,losses}$.

$$P_{or2,losses} = \frac{\omega_{slip,2}}{p} T_{g2} \tag{2.18}$$

where

$$\omega_{slip,2} = p(\omega_{g2} - \omega_{m2}) \tag{2.19}$$

In this case, the stator of the machine is stationary so ω_{g2} is found as

$$\omega_{g2} = \omega_s \tag{2.20}$$

.

where ω_s is defined as the stator frequency.

If this system was left as is, it would still show efficiency improvements over today's starter and alternator. But, the package is very large and heavy. To address these problems, Hoeijmakers and Ferreira presented a new power conversion unit, the EVT.

2.5 The Electric Variable Transmission

If the restriction that the rotor slip frequencies, ω_{or}, of both machines are kept equal is imposed, the size of the yokes on the shared rotor can be greatly reduced. This is due to the fact that in an induction machine, the torque developed is essentially a function of the frequency of the rotor currents and the square of the flux density. If both machines are operating with the same rotor current frequency, they can essentially share the rotor currents.

The thinning of the yokes changes the electromagnetic behavior of the EVT. The thin yokes cause the shared rotor of the machine to saturate much quicker then in the concentric implementation. This causes an interesting interaction between the two machines. As the shared rotor starts to saturate, a portion of the flux generated in the inner rotor of the first machine will be passed directly to the stator of the second

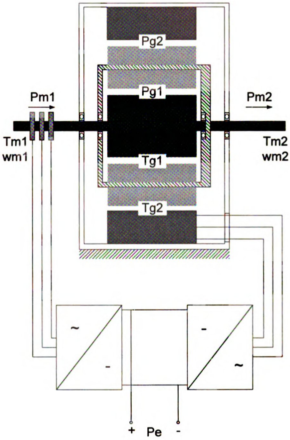

Figure 2.5. The Electric Variable Transmission

machine.

This interaction produces another torque component to consider when studying the EVT. This torque, T_{rs}, adds another component to the air gap torque of machine 1.

$$T_{g1} = T_{m1} - T_{rs} \tag{2.21}$$

CHAPTER 3

Analysis Methods

3.1 Introduction

In the previous section it was stated that the EVT was essentially two concentric induction machines with a shared rotor. When the power flow through the machine was developed, it was done so as a pair of traditional induction machines with some added complexity due to the shared outer rotor. This method will be used to develop the model for the EVT.

The first step is developing a set of equations that can be used to determine the machine parameters. Once a set of equations has been established, a method for finding the necessary values to solve those equations will be developed. In this chapter the methods and equations for calculating electrical parameters for the EVT using finite element analysis will be developed.

3.2 Resistances

The first machine parameter investigated will be the resistance. The resistance of a wire can be found using the formula,

$$R = \frac{\rho l}{A} \tag{3.1}$$

where ρ is the resistivity of the material, l is the length of the wire and A is the cross sectional area of the wire. This equation can be applied directly to the rotor bars since they can be treated as a single strand of wire.

Equation (3.1) can be modified slightly to take into account the number of windings found in each of the inner rotor and stator slots. If it is assumed that the slots are completely filled with wire, then the cross sectional area of a single strand of wire can be found by dividing the area of the slot by the number of windings.

$$A = \frac{A_{slot}}{N} \tag{3.2}$$

where A_{slot} is the cross sectional area of the slot and N is the number of windings contained in the slot.

This is not the case. Stacking round wires on top of each other causes small airgaps in the slot. A correction factor can be introduced to account for the small airgaps. This factor will be referred to as the fill factor, η. The total resistance in the slot can then be found by multiplying the number of windings in the slot by the resistance of one winding and dividing by the fill factor.

$$R = N^2 \frac{\rho l}{\eta A_{slot}} \tag{3.3}$$

3.3 Stator and Inner Rotor Self and Mutual Inductances

Since the EVT is essentially two concentrically arranged induction machines, analysis can be started using the voltage equations for a traditional induction machine. Equations (3.4) through (3.9) are the voltage equations for a traditional induction machine where the rotor can be represented by balanced three phase windings.

$$v_{as} = r_s i_{as} + \frac{d\lambda_{as}}{dt} \tag{3.4}$$

$$v_{bs} = r_s i_{bs} + \frac{d\lambda_{bs}}{dt} \tag{3.5}$$

$$v_{cs} = r_s i_{cs} + \frac{d\lambda_{cs}}{dt} \tag{3.6}$$

$$v_{ar} = r_r i_{ar} + \frac{d\lambda_{ar}}{dt} \tag{3.7}$$

$$v_{br} = r_r i_{br} + \frac{d\lambda_{br}}{dt} \tag{3.8}$$

$$v_{cr} = r_r i_{cr} + \frac{d\lambda_{cr}}{dt} \tag{3.9}$$

For the implementation to be used in this investigation, there will not be balanced three phase outer rotor windings. Therefore, the self and mutual inductance of the stator and inner rotor will first be discussed and the outer rotor will be ignored for the moment. For the remainder of this section, it will be assumed that there are no outer rotor bars. Equations (3.4) through (3.9) can be modified to represent the coils in an EVT with no outer rotor bars.

$$v_{as} = r_s i_{as} + \frac{d\lambda_{as}}{dt} \tag{3.10}$$

$$v_{bs} = r_s i_{bs} + \frac{d\lambda_{bs}}{dt} \tag{3.11}$$

$$v_{cs} = r_s i_{cs} + \frac{d\lambda_{cs}}{dt} \tag{3.12}$$

$$v_{air} = r_{ir} i_{air} + \frac{d\lambda_{air}}{dt} \tag{3.13}$$

$$v_{bir} = r_{ir} i_{bir} + \frac{d\lambda_{bir}}{dt} \tag{3.14}$$

$$v_{cir} = r_{ir} i_{cir} + \frac{d\lambda_{cir}}{dt} \tag{3.15}$$

The flux linkage for a traditional machine would follow the form of λ_{as} found in equation (3.16).

$$\lambda_{as} = L_{asas} i_{as} + L_{asbs} i_{bs} + L_{ascs} i_{cs} + L_{asar} i_{ar} + L_{asbr} i_{br} + L_{ascr} i_{cr} \tag{3.16}$$

Similar to the voltage equations, the flux linkage equations could be modified to represent an EVT with no outer rotor bars. The flux linkages for the EVT without outer rotor bars can be described in equations with the same form of λ_{as}, found in the following equation.

$$\lambda_{as} = L_{asas} i_{as} + L_{asbs} i_{bs} + L_{ascs} i_{cs} + L_{asair} i_{air} + L_{asbir} i_{bir} + L_{ascir} i_{cir} \tag{3.17}$$

If current is applied only to one coil, then the flux linkage equation (3.17) becomes much simpler for each flux linkage. Since all of the other currents are zero, only one term is left on the right side of equation (3.17). Equation (3.18) describes λ_{bir} when current is applied only to the phase B coil of the inner rotor.

$$\lambda_{bir} = L_{birbir} i_{bir} \tag{3.18}$$

If saturation is neglected, then the inductance can be assumed to be constant.

With this in mind, equation (3.18) can be inserted into equation (3.14) for λ_{bir}.

$$v_{bir} = r_{ir} i_{bir} + \frac{d}{dt} L_{birbir} i_{bir} \tag{3.19}$$

Equation (3.19) can now be solved for L_{birbir} using phasor notation. This same method could be used to find the self inductance of any inner rotor or stator coil.

Finding the mutual inductances in the inner rotor or stator is very similar to finding the self inductance of one of the inner rotor or stator coils. The voltage equations (3.10 - 3.15) along with the flux linkage equations of the form of equation (3.17) would remain the same when looking for the mutual inductance in the inner rotor or the stator. In fact, the mutual inductance between coils within one member or between coils in different members can be found using the same method.

If current is applied to one coil in either the inner rotor or stator, equations of the form of equation (3.17) can be found for all of the other coils in that member and in the other members. The resulting equations would be simpler then equation (3.17) since all but one of the currents would be zero. If a current was applied to the phase b coil of the inner rotor, the flux linkage equations would be as follows and would remain in this same form if current were applied to a different coil.

$$\lambda_{as} = L_{asbir} i_{bir} \tag{3.20}$$

$$\lambda_{bs} = L_{bsbir} i_{bir} \tag{3.21}$$

$$\lambda_{cs} = L_{csbir} i_{bir} \tag{3.22}$$

$$\lambda_{air} = L_{airbir} i_{bir} \tag{3.23}$$

$$\lambda_{cir} = L_{cirbir} i_{bir} \tag{3.24}$$

As was done in order to find the self inductance, the flux linkage values found after applying the current to a single coil could be substituted into the voltage equations (3.10 - 3.15). The resulting equations could then be solved for the mutual inductances using phasor notation. Continuing with the example from earlier, the voltage equations necessary to find the mutual inductance between the phase b coil of the inner rotor and all other coils would be as in equations (3.25) through (3.29).

$$v_{as} = \frac{d}{dt} L_{asbir} i_{bir} \tag{3.25}$$

$$v_{bs} = \frac{d}{dt} L_{bsbir} i_{bir} \tag{3.26}$$

$$v_{cs} = \frac{d}{dt} L_{csbir} i_{bir} \tag{3.27}$$

$$v_{air} = \frac{d}{dt} L_{airbir} i_{bir} \tag{3.28}$$

$$v_{cir} = \frac{d}{dt} L_{cirbir} i_{bir} \tag{3.29}$$

This same method could be used to find the mutual inductance of any inner rotor or stator coil with all other coils in the inner rotor and stator.

3.4 Outer Rotor Self and Mutual Inductances

The outer rotor bars need to be handled differently then the inner rotor and stator coils. Since the outer rotor will consist of a set of cast aluminum rotor bars and not three sinusoidal distributed coils, one rotor bar cannot be treated as one coil. This is not the only issue concerning finding the inductances associated with the outer rotor. The other problem comes in the fact that the rotor bars are not isolated from each other. The rotor bar ends are all connected in the actual cast rotor.

To avoid these issues, the outer rotor must be investigated in a different manner. The outer rotor can be looked at as a set of current carrying loops bounding closed regions[7]. Figure 3.1 illustrates this concept.

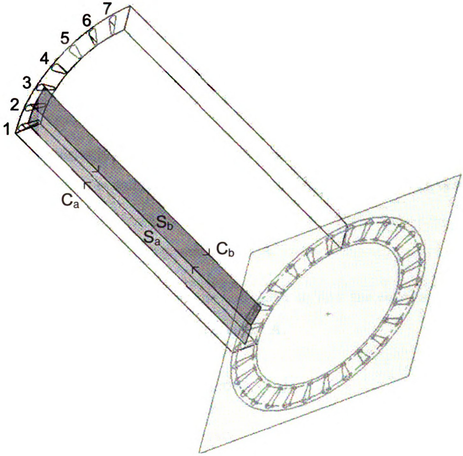

Figure 3.1. The outer rotor with regions S_a and S_b

Closed loop C_a consists of a path down the center of rotor bars one and two and the rotor rings at both ends of the rotor. Closed loop C_a bounds the surface S_a. Similarly, closed loop C_b encloses surface S_b and is comprised of rotor bars 2 and 3 and the rotor rings. For the sake of this investigation, it is assumed that current is uniformly distributed throughout the rotor bars and rotor rings. If a current I flows through C_a, a magnetic field $\mathbf{B_a}$ will be created.

The magnetic flux Φ is related to the magnetic flux density $\mathbf{B}$ through a given area bounded by a closed path C through the following equation

$$\Phi = \int_{S} \mathbf{B} \cdot ds. \tag{3.30}$$

The vector magnetic potential, $\mathbf{A}$, can be used to find the inductances. The magnetic vector potential is defined such that the magnetic flux density, $\mathbf{B}$, is expressed as the curl of $\mathbf{A}$.

$$\mathbf{B} = \nabla \times \mathbf{A} \tag{3.31}$$

Equations (3.30) and (3.31) can be combined to find the relationship between magnetic flux Φ and magnetic vector potential $\mathbf{A}$.

$$\Phi = \int_{S} \nabla \times \mathbf{A} \cdot ds \tag{3.32}$$

By applying Stoke's theorem to equation (3.32) the equation can be further reduced to

$$\Phi = \oint_{C} \mathbf{A} \cdot dl. \tag{3.33}$$

Equation (3.33) states that the line integral of $\mathbf{A}$ around any closed path is equal to the total flux passing through the area enclosed by the path. If equation (3.33) is applied to the closed path C_a the total flux passing through S_a can be found. Similarly, equation (3.33) can be applied to any set of rotor bars creating a closed path and used to calculate the flux passing through that path.

A coordinate system can be established to investigate the surface S_a as was described in Figure 3.1. The y-axis, y_a, will run down the height of the rotor bar. The x-axis, x_a, runs along the straight path connecting the centers of rotor bars one and two. Figure 3.2, displays surface S_a in reference to this coordinate system.

If a current is applied such that the current in rotor bar one flows in the positive y_a direction and the current in rotor bar two flows in the negative y_a direction, the magnetic vector potential **A** will only have a y_a component. In light of this decision, **A** can be defined to have a line integral from 0 to h. This will simplify equation (3.33) to a single integral in the x_a direction.

$$\Phi_a = \int_0^w A_{y_a} dx_a \tag{3.34}$$

A_{y1} can be established as the magnetic vector potential from the point (0,0) to (0,h) as is described in Figure 3.2. Similarly, A_{y2} can be established as the magnetic vector potential from the point (w,0) to (w,h). Equation (3.34) can now be solved to give the flux passing through the surface S_a.

$$\Phi_a = (A_{y1} - A_{y2})w \tag{3.35}$$

Equation (3.35) can be applied to all of the surfaces S as long it is adjusted for the rotor bars involved.

The Biot-Savart Law states that the flux Φ in a magnetic material of constant permeability will have linear relationship to current through the value inductance L.

$$\Phi = LI \tag{3.36}$$

This holds true for the case where there exists only one winding in the closed loop C.

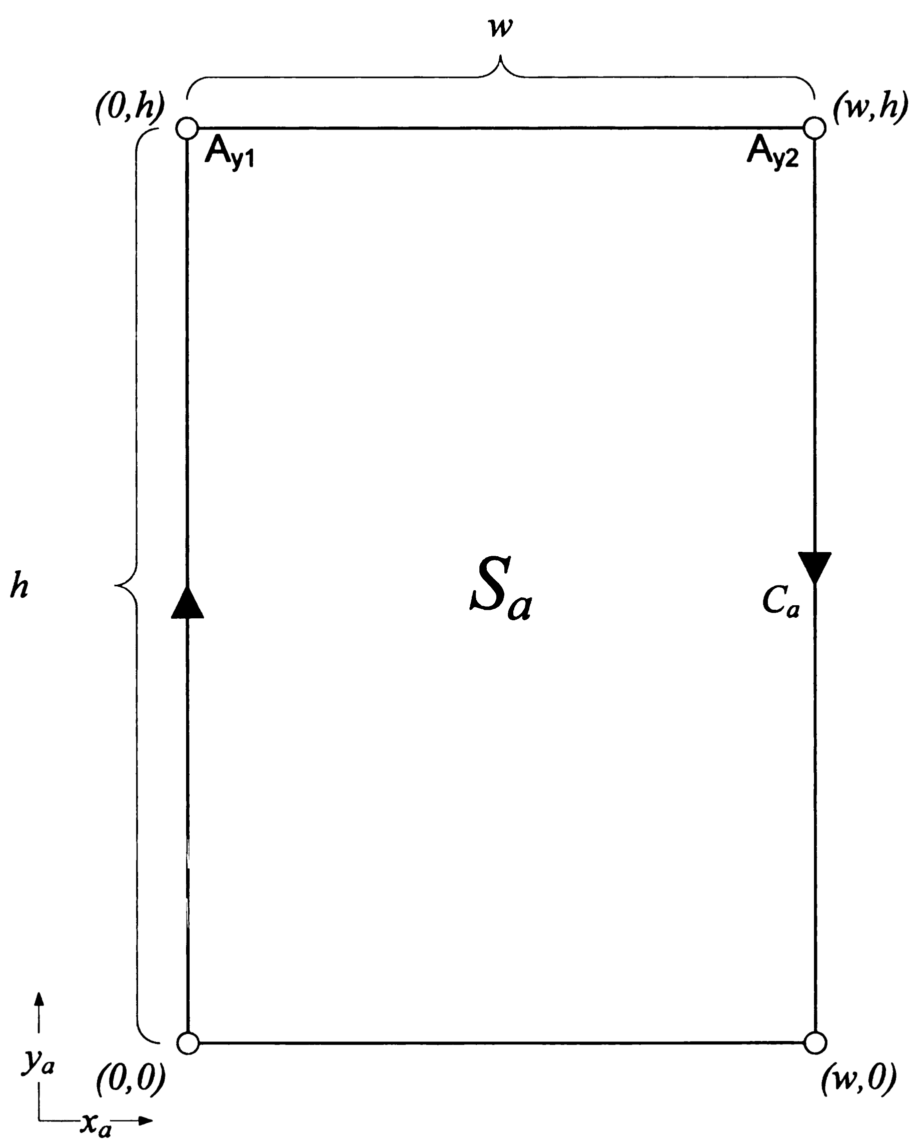

Figure 3.2. Region S_a enclosed by closed loop C_a

In the case of multiple windings equation (3.36) can be related to the flux linkage λ

$$\lambda = N\Phi \tag{3.37}$$

where N is the number of turns in the closed loop C.

$$\lambda = LI \tag{3.38}$$

In this case there will only exist one winding so, equation (3.36) can be used to find the inductance.

$$L = \frac{\Phi}{I} \tag{3.39}$$

If it is assumed that the permeability of rotor bars does not change with I, the self inductances of the closed loops C can be found by applying equation (3.39) directly. For example, to find the self inductance of C_a equation (3.39) would be represented as

$$L_{aa} = \frac{\Phi_{aa}}{I_a} \tag{3.40}$$

where I_a is the current in bars one and two.

The equation for finding the mutual inductance for two surfaces is very similar to that of the self inductance. For example, the mutual inductance between surfaces S_a and S_b could be investigated. If a current I_a flows through the closed path C_a, a magnetic field $\mathbf{B_a}$ will be created. Some of the magnetic flux due to $\mathbf{B_a}$ will link with the surface S_b. This flux can be found by using an equation of the form of equation (3.41) when current is applied to rotor bars one and two.

$$\Phi_{ab} = (A_{y2} - A_{y3})w \tag{3.41}$$

The mutual inductance can then be found as it was in the case of the self inductance by dividing by the current applied to rotor bars one and two, I_a.

$$L_{ab} = \frac{\Phi_{ab}}{I_a} \tag{3.42}$$

3.5 Stator and Inner Rotor to Outer Rotor Inductances

In Section 3.3 the outer rotor was excluded because it did not consist of three sinusoidally windings. Therefore, a different method than the one developed in Section 3.3 must be used to find the stator and inner rotor to outer rotor mutual inductances. The method developed in the last section could be used instead. By applying current to the stator and inner rotor, the flux due to those currents in the rotor bars could be calculated by measuring the magnetic vector potential in specific locations in the outer rotor.

Current can be applied to the stator one phase at a time and then to the inner rotor one phase at a time. Then equations of the form of equation (3.35) can be applied to find the flux passing through the outer rotor surfaces. Once the flux through the surfaces is known, equations (3.37) and (3.38) can be combined to find the inductance in the rotor loops caused by the stator and inner rotor windings.

$$L = \frac{N\Phi}{I} \tag{3.43}$$

For example, if a current were applied to phase A of the stator an equation of the form of equation (3.41) could be used to find the flux in the region enclosed by C_b. Equation (3.43) could then be modified as follows to find the mutual inductance between phase a of the stator and the outer rotor region S_b

$$L_{asbor} = \frac{N\Phi_{asbor}}{I_{as}}. \tag{3.44}$$

Equation (3.44) could be modified to find any mutual inductance between the stator or inner rotor and the outer rotor.

CHAPTER 4

Simulation Setup and Results

4.1 FEA Setup

In the last chapter, a set of equations was developed to find the machine parameters necessary for the EVT model. In this chapter, a set of simulations to find the parameters necessary to solve those equations will be developed. Finite element analysis will be used to simulate a given geometry and then the results of that simulation will be analyzed to find the necessary parameters.

4.2 Simulation Geometry

A smaller overall geometry will be used then that presented in the Hoeijmakers and Ferreira paper[4]. This will be done to help facilitate any future work using an actual prototype part as a smaller machine should be less costly to have manufactured and would be able to be operated with lower supply current. Since the actual dimensions of the EVT are not known, a new geometry will be created. The overall machine diameter will be set to 198.5 mm with an outer rotor thickness of 19 mm and 0.25 mm air gaps. The depth of the machine will be set at 235 mm. Appendix A.6 contains detailed drawings of the machine geometry.

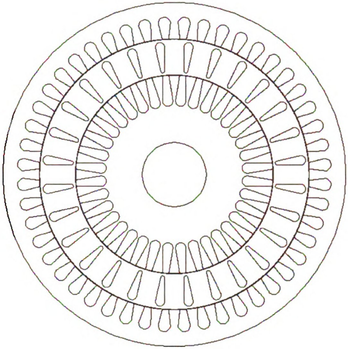

Figure 4.1. Full EVT geometry

The 4 pole induction machine will consist of 28 outer rotor bars, 36 inner rotor slots and 48 stator slots. One quarter of the machine will be modeled to help reduce simulation time. Figure 4.2 is a representation of the EVT geometry to be analyzed.

Since the purpose of this thesis is to create a linear model, the saturation effect described in Section 2.5 will not be modeled. Instead, the effect will be simulated by allowing a small amount of flux to link the stator to the inner rotor. The amount of flux linking the stator and inner rotor is determined largely by the outer rotor geometry. Originally, a geometry was chosen with 44 outer rotor bars instead of 28. This geometry resulted in too much flux linking the stator to the inner rotor. The outer rotor geometry was modified until a small amount flux linked the stator and outer rotor.

The material selected for the stator and inner and outer rotors was iron. When solving for the inductances, the material for the rotor bars and coils was selected as

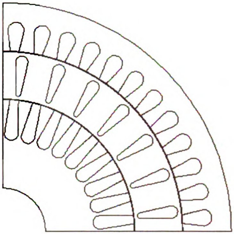

Figure 4.2. The EVT geometry created to perform FEA analyis

vacuum.

The program chosen for the FEA analysis, Flux2D, only allows for one airgap to be represented as a rotating airgap. Therefore, the rotating airgap will be set according to where current or voltage is applied. If power is applied to an inner rotor coil, then the inner airgap will be set as rotating. If a stator coil is powered, then the outer airgap will rotate. If power is applied to an outer rotor bar, then the outer airgap is set as the rotating airgap. The non rotating airgap will be set as vacuum in all these cases.

4.3 Resistance Calculation Setup

All of the resistances in the EVT can be found using equation (3.3). In order to solve for the stator and inner rotor winding resistances and rotor bar resistances, the physical characteristics outlined in equation (3.3) must be found. The overall physical dimensions are the same as those defined in Section 4.2 and Appendix A.6.

Since the rotor bars are a single conductor, the number of turns is $N_{or} = 1$ and the fill factor is $\eta = 1$. The resistivity is a material dependent value. Since the outer rotor will be made out of aluminum, the resistivity will be set as $\rho_{or} = 2.78 \times 10^{-8}\Omega m$. The length of the rotor bars is simply the depth of the machine, $l = 235mm$. The area of the rotor bar can be found using geometry but, for simplicity, the FEA tool will be used to find the area of the outer rotor bar.

The number of turns for the inner rotor windings will be established as $N_{ir} = 44$. Since the inner rotor slots will be filled with copper windings, the fill factor will be set to $\eta = 0.8$ and the resistivity of the inner rotor windings will be set as $\rho_{ir} = 1.72 \times 10^{-8}\Omega m$. The length of the inner rotor windings is the same as that established for the outer rotor bars, $l = 235mm$. To determine the area of the inner rotor slots we will again rely on the FEA tool as we did for the outer rotor bars.

The same number of windings will be used for the stator as were used for the inner rotor, $N_s = 44$. The fill factor for the stator will be set to $\eta = 0.8$ as it was for the inner rotor. The resistivity of the stator windings will be set as $\rho_s = 1.72 \times 10^{-8}\Omega m$ since the stator slots will be filled with copper windings. Again, the length of the stator windings is the same as that established for the outer rotor bars, $l = 235mm$. To determine the area of the stator slots, the FEA tool will again be used.

4.4 Stator and Inner Rotor Setup

To find the currents and voltages needed to calculate the inductance due to the stator and inner rotor windings a transient magnetic analysis will be run. A transient magnetic analysis was chosen because a steady state analysis would not have accounted for the time varying signal needed as described in equations of the form of equation (3.19). The geometry and machine parameters described in Section 4.2 will be used in all of the analyses.

For the analyses, the coils in the circuit will be wired in a wye topology. A resistance of 0.5575 Ω will be added in series with each of the sets of coils to simulate

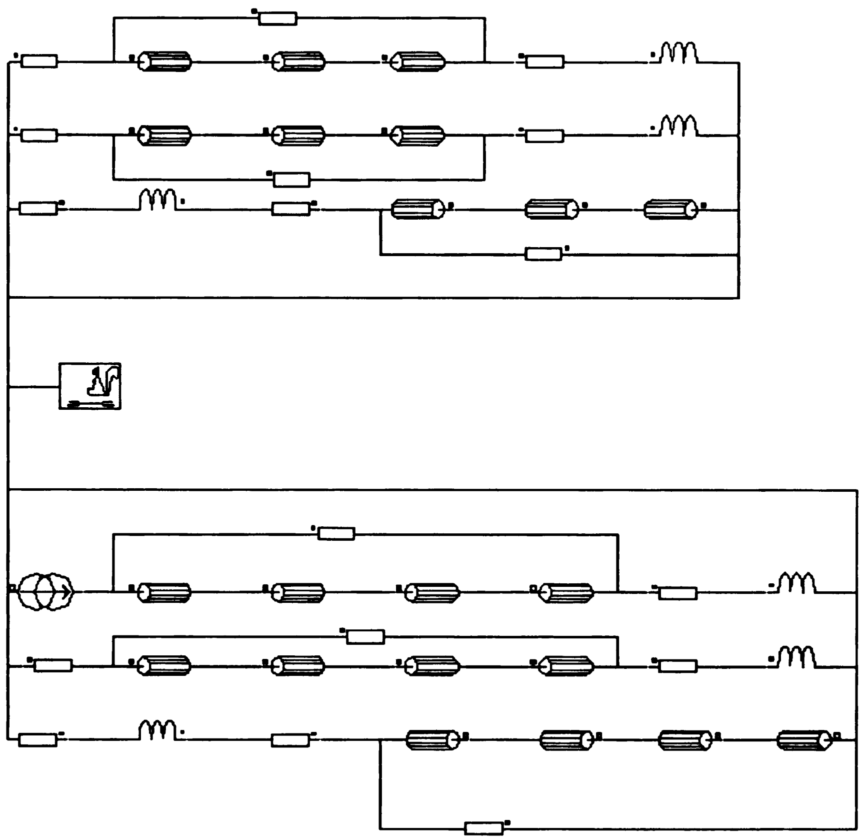

Figure 4.3. Circuit used to find self and mutual inductance of phase A of the stator.

the end winding resistance. Similarly, a 2.1 mH inductor will also be wired up in series with the coils to simulate end inductance. One coil will be fed with 0.1 A current at 60 Hz. A low current was chosen so that the iron in the stator and both rotors would not saturate. All of the other coil sets will have a large resistance, 40 kΩ, wired in series with the coils to simulate an open circuit. The coil resistances will be set as described in the previous section. A large parallel resistor, 20 kΩ, will be added to each coil set to measure the voltage in each phase. Figure 4.3 is an example of the type of circuit to be used. In this case, the current supply is connected to phase A of the stator. For the simulations where current will be applied to other coils, the current supply would be moved to the phase of interest and all other coils will have a large resistance, 40 kΩ, set in series with them.

The rotor bars will be wired up as a squirrel cage. The end resistance of the squirrel cage will be set at 40 kΩ to isolate the rotor bars from each other. The end inductance of the squirrel cage will be set at 4 nH.

In total, 6 simulations will be run; one each with one set of coils being fed in either the inner rotor or the stator. The angular velocity in the rotating airgap will be set to 0 rpm. The current source will be set to create a sinusoidal current with a frequency of 60 Hz and a phase angle of 0°.

4.5 Outer Rotor Setup

In Section 3.4, equations (3.40) and (3.42) were derived for calculating the self and mutual inductance of the outer rotor. In both equations there are no time varying components. Since there are no time varying components, a magneto-static analysis was performed on the EVT to find the values necessary to calculate the inductances associated with the outer rotor.

The geometry described in Section 4.2 was used to simulate the EVT. A magneto-static analysis does not require a circuit as was used in Section 4.4. Instead, current is applied directly to regions where the current would flow. For the first analysis of the EVT, the simulation will be run with current, $I_1 = 0.1A$, applied to rotor bar 1 and the opposite current, $I_2 = -0.1A$, to rotor bar 2. The current was kept low as it was in the stator and inner rotor inductance simulations in order to avoid saturation of the iron components. For the next simulation, positive current will be applied to rotor bar 2 and negative current to rotor bar 3. Simulations will be repeated in this manner until current is applied to rotor bar 7 and the opposite current to rotor bar 1. This will result in 7 total simulations in order to find all of the necessary magnetic vector potential values.

CHAPTER 5

Analysis Results

5.1 Resistance Results

In Section 4.3, most of the values necessary to calculate the resistances of all of the windings and rotor bars in the EVT were established. The last value needed to calculate the resistances was the area of each of the regions. Table 5.1 shows the results for the area measurements from the FEA. It also shows the results of applying these values and the values established in Section 4.3 to equation (3.3) to find the resistances of the windings and rotor bars.

Region	Area (mm^2)	Fill Factor	Resistance (Ω)
Stator Winding	72	0.8	0.1359
Inner Rotor Winding	87.715	0.8	0.1115
Outer Rotor Bar	68.95	1	9.783×10^{-5}

Table 5.1. Winding and Rotor Bar Resistances

	Current Applied To					
	SA	SB	SC	IRA	IRB	IRC
SA	20.83	8.505	8.544	0.732	0.360	0.363
SB	8.505	20.83	8.544	0.360	0.732	0.363
SC	8.544	8.544	20.82	0.360	0.360	0.738
IRA	0.834	0.417	0.404	9.667	3.964	3.931
IRB	0.417	0.834	0.404	3.964	9.667	3.931
IRC	0.410	0.410	0.836	3.931	3.931	9.663

Table 5.2. Stator and inner rotor voltages (V) when current was applied to a set of windings.

5.2 Stator and Inner Rotor FEA Results

After the six simulations described in Section 4.4 were complete, the voltage across all of the coils in the stator and inner rotor were measured. Figures 5.1 and 5.2 show the voltages measured in all of the windings when current was applied to one phase of the stator or inner rotor respectively. In order to perform the calculations described in Section 3.3, the magnitude of all of the voltages must be found. This can be done by performing an FFT on each voltage curve and then selecting the first harmonic value. Table 5.2 contains the results of those measurements. These voltages will be used to find the self and mutual inductances of the stator and inner rotor windings. Since a current was applied directly to the windings, the current in all of the calculations will be $I = 0.1A$.

In Section 3.3, it was stated that if a voltage is applied to one set of windings in the inner rotor or stator, equations of the form of equation (3.19) could be used to calculate the self inductance of that set of windings. Equations of the form of equation (3.19) can be represented using complex notation to illustrate the relationship between the voltage and inductance.

$$V_{bir} = I_{bir}(R_{ir} + X_{bir}) \tag{5.1}$$

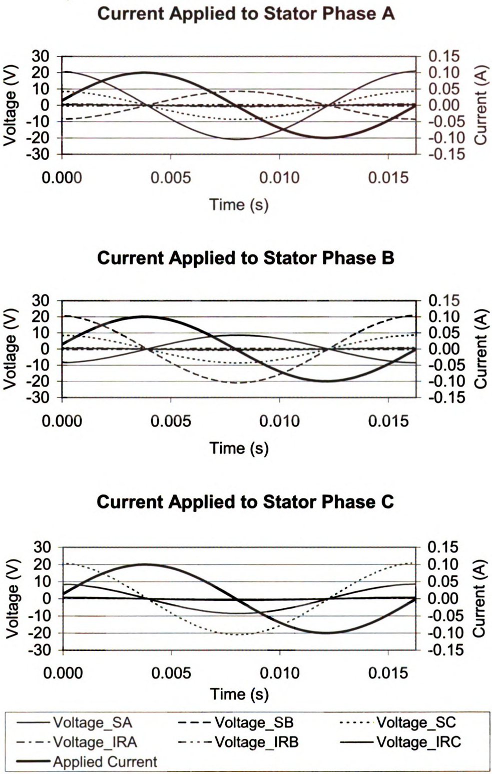

Figure 5.1. Stator and inner rotor voltages (V) measured when current was applied to one stator phase.

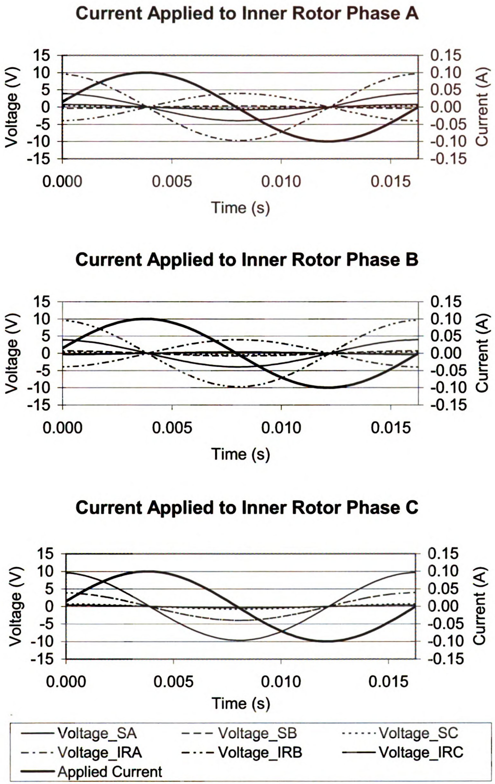

Figure 5.2. Stator and inner rotor voltages (V) measured when current was applied to one inner rotor phase.

	Current Applied To					
	SA	SB	SC	IRA	IRB	IRC
SA	553	226	227	19.4	9.54	9.63
SB	226	553	227	9.54	19.4	9.63
SC	227	227	552	9.53	9.53	19.6
IRA	22.1	11.1	10.7	256	105	104
IRB	11.1	22.1	10.7	105	256	104
IRC	10.8	10.8	22.2	104	104	256

Table 5.3. Stator and inner rotor inductances (mH).

Since all of the voltage measurements made on the phases where current was applied in Figures 5.1 and 5.2 are 90°out of phase with respect to the current, it can be assumed that the resistance in equation (5.1) has a negligible effect. Therefore, the reactance can be found by dividing the magnitude of the measured voltage by the magnitude of the applied current.

$$X_{bir} = \frac{V_{bir}}{I_{bir}} \tag{5.2}$$

With the reactance calculated, the inductance can be found by dividing the reactance by the frequency of the voltage.

$$L_{bir} = \frac{X_{bir}}{\omega} \tag{5.3}$$

Equations (5.2) and (5.3) could easily be modified for the case where current is applied to any single stator or inner rotor phase.

Since equations of the form of equations (3.25 - 3.27) do not include resistance, equations of the form of equations (5.2) and (5.3) can be modified to find the mutual inductances in the stator and inner rotor. Following the example where current is applied to phase B of the inner rotor, the mutual inductance between phase B of the inner rotor and phase A in the stator could be found using equations (5.4) and (5.5).

	A	B	C
A	553	226	227
B	226	553	227
C	227	227	552

Table 5.4. Stator self and mutual inductances (mH).

	A	B	C
A	256	105	104
B	105	256	104
C	104	104	256

Table 5.5. Inner Rotor self and mutual inductances (mH).

Equations of this form could be used to find the mutual inductance between any set of inner rotor or stator coils.

$$X_{biras} = \frac{V_{as}}{I_{bir}} \tag{5.4}$$

$$L_{biras} = \frac{X_{biras}}{\omega} \tag{5.5}$$

Table 5.3 establishes the self and mutual inductances between stator and inner rotor at a fixed position. This is appropriate for stator to stator mutual inductance and the inner rotor to inner rotor mutual inductance as their relative position cannot change. Tables 5.4 and 5.5 detail these values.

For the inductances between the two members, the inductance values need to be found without respect to position. This can be done by dividing the values found in Table 5.3 by the cosine of the angle between the phase where the voltage was applied and where the current was measured. Table 5.6 and 5.7 detail the results of this

	SA	SB	SC
IRA	19.4	-19.1	-19.3
IRB	-19.1	19.4	-19.3
IRC	-19.1	-19.1	19.6

Table 5.6. Stator to inner rotor mutual inductances (mH).

	IRA	IRB	IRC
SA	22.1	-22.1	-21.5
SB	-22.1	22.1	-21.4
SC	-21.7	-21.7	22.2

Table 5.7. Inner rotor to stator mutual inductances (mH).

modification.

It will be useful to have a single value for the self and mutual inductances instead of a table of values. The mutual inductance of the stator or inner rotor can be found by first averaging the off-diagonal values of the stator and inner rotor self and mutual inductance tables, Tables 5.4 and 5.5. The average values can then be multiplied by 2, resulting in the mutual inductances. This differs from a traditional induction motor because when the reactance was found, only the magnitude was found. If the reactance had been found including the angle of the voltage, the final value would need to be multiplied by -2.

$$L_s = 453mH \tag{5.6}$$

$$L_{ir} = 209mH \tag{5.7}$$

The leakage inductance can be found by averaging the diagonal values of the stator and inner rotor self and mutual inductances tables, Tables 5.4 and 5.5. And then subtracting the mutual inductances found above, equations (5.6) and (5.7), from

	Rotor Bar with positive current						
	1	2	3	4	5	6	7
Rotor Bar 1	18.2	1.79	0.446	0.344	0.453	1.79	18.3
2	-18.2	18.3	1.79	0.446	0.352	0.45	1.78
3	-1.78	-18.3	18.3	1.79	0.453	0.348	0.441
4	-0.448	-1.79	-18.3	18.3	1.79	0.45	0.34
5	-0.348	-0.453	-1.79	-18.3	18.3	1.79	0.441
6	-0.449	-0.352	-0.446	-1.79	-18.3	18.3	1.78
7	-1.78	-0.453	-0.344	-0.446	-1.8	-18.3	18.3

Table 5.8. Magnetic vector potential (μWb/m) of rotor bars when current is applied to two bars.

the resultant value.

$$L_{ls} = 100mH \tag{5.8}$$

$$L_{lir} = 47.2mH \tag{5.9}$$

Finally, the mutual inductance between the stator and inner rotor can be found averaging the magnitudes of all of the mutual inductances found in Tables 5.6 and 5.7.

$$Lsir = Lirs = 20.6mH \tag{5.10}$$

5.3 Outer Rotor FEA Results

After a total of 7 simulations were run, the magnetic potential was measured in the center of each of the rotor bars. This was done to create regions S_a through S_g as was described in Section 3.4. Table 5.8 contains the magnetic vector potential measured in each of the rotor bars. The table is arranged such that the columns correspond to the rotor bar where positive current was applied and the rows correspond to the rotor bar where the magnetic vector potential was measured.

		Rotor Region						
		1	2	3	4	5	6	7
Rotor Region	A	0.5624	-0.2551	-0.0208	-0.0016	0.0016	0.0207	0.2552
	B	-0.2537	0.5655	-0.2551	-0.0208	-0.0016	0.0016	0.0207
	C	-0.0206	-0.2551	0.5655	-0.2551	-0.0207	-0.0016	0.0016
	D	-0.0015	-0.0207	-0.2551	0.5655	-0.2551	-0.0207	-0.0016
	E	0.0016	-0.0016	-0.0208	-0.2551	0.5655	-0.2551	-0.0207
	F	0.0206	0.0016	-0.0016	-0.0208	-0.2549	0.5655	-0.2552
	G	0.2536	0.0207	0.0016	-0.0016	-0.0208	-0.2551	0.5655

Table 5.9. Magnetic flux (μWb) of regions enclosed by rotor bars when current is applied to two bars.

The values in Table 5.8 can be used to calculate the flux passing through each of the rotor regions S_a through S_g. Equations of the form of equation (3.35) can then be used to calculate the flux passing through the regions. Table 5.9 contains the resulting magnetic flux from these calculations.

Finally, the self and mutual inductances of the rotor regions can be found by dividing the magnetic flux in the region by the current applied to the rotor bars, $I = 0.1A$ as was described in equations (3.40) and (3.42). Table 5.10 contains the inductances found by applying this method. The self inductances are listed along the diagonal and mutual inductances are found throughout the rest of the table.

It would be useful to have a single value for the mutual inductance in the outer rotor as well as the rotor leakage inductance. The mutual inductance can be found by first finding the inductances in Table 5.10 regardless of position. This can be done by dividing all of the values in the table by the relative angle to where the current was applied. The mutual inductance of the outer rotor loops can then be found by taking the average of the off diagonal values.

$$L_{or} = 1.679\mu H \tag{5.11}$$

	Rotor Region						
	1	2	3	4	5	6	7
Rotor Region A	5.6238	-2.5508	-0.2076	-0.0158	0.0156	0.2070	2.5523
B	-2.5369	5.6547	-2.5508	-0.2076	-0.0156	0.0158	0.2069
C	-0.2058	-2.5508	5.6547	-2.5508	-0.2066	-0.0158	0.0156
D	-0.0155	-0.2066	-2.5508	5.6547	-2.5508	-0.2070	-0.0156
E	0.0156	-0.0156	-0.2076	-2.5508	5.6547	-2.5508	-0.2069
F	0.2056	0.0156	-0.0158	-0.2076	-2.5493	5.6547	-2.5523
G	2.5369	0.2066	0.0158	-0.0158	-0.2081	-2.5508	5.6547

Table 5.10. Self and mutual inductance (μH) of regions enclosed by two rotor bars.

The leakage inductance of the outer rotor loops can be found by taking the average of the diagonal values of the inductance area found in the previous step and then subtracting off the mutual inductance.

$$L_{lor} = 3.972\mu H \tag{5.12}$$

5.4 Outer Rotor to Stator and Inner Rotor FEA Results

To find the mutual inductances between the outer rotor and the stator and inner rotor, the simulations described in Section 4.4 and used in Section 5.2 can be used. The magnetic vector potential in the center of each rotor bar was measured for each of the six simulations. Figures 5.3 and 5.4 shows the magnetic vector potential measured in the center of each of the rotor bars when current was applied to a single phase of the stator or inner rotor. In order to perform the calculations described in Section 3.5, the magnitude of the magnetic vector potentials must be found. To find these values, each measurement point can be divided by the sine of the frequency of the waveform multiplied by the time at each point. This should result in the instantaneous

	Winding					
Rotor Region	SA	SB	SC	IRA	IRB	IRC
A	179.9	-122.9	33.1	84.4	-58.6	15.5
B	189.7	-55.7	100.2	88.5	-26.9	47.5
C	143.9	11.8	165.3	67.5	5.6	77.8
D	78.2	78.2	192.6	37.1	37.1	90.4
E	11.8	143.9	165.3	5.6	67.5	77.8
F	-55.8	189.7	100.2	-26.9	88.5	47.5
G	-122.9	179.9	33.0	-58.6	84.4	15.5

Table 5.11. Rotor bar vector potential (μWb/m) when current is applied to inner rotor or stator windings.

	Winding					
Rotor Region	SA	SB	SC	IRA	IRB	IRC
A	-0.1525	-1.0375	-1.0380	-0.0639	-0.4889	-0.4935
B	0.7086	-1.0434	-1.0056	0.3241	-0.5027	-0.4679
C	1.0155	-1.0255	-0.4211	0.4703	-0.4863	-0.1952
D	1.0254	-1.0154	0.4211	0.4863	-0.4703	0.1952
E	1.0435	-0.7086	1.0055	0.5026	-0.3241	0.4679
F	1.0374	0.1525	1.0381	0.4889	0.0638	0.4935
G	0.8801	0.8801	1.0212	0.3983	0.3982	0.4801

Table 5.12. Outer Rotor Magnetic Flux (μWb) when current is applied to the stator and inner rotor.

magnitude of the signal. The resulting values can be averaged to find the average magnitude of the signal. Table 5.11 contains the results of those measurements.

The values in Table 5.11 can be used to calculate the flux passing through each of the rotor regions S_a through S_g. This can be done by using the same method as was used to find the outer rotor bar self and mutual inductances. Equations of the form of equation (3.35) can be used to calculate the flux passing through the rotor bar regions. Table 5.12 contains the flux resulting from that calculation.

The mutual inductance between the stator and inner rotor to the outer rotor

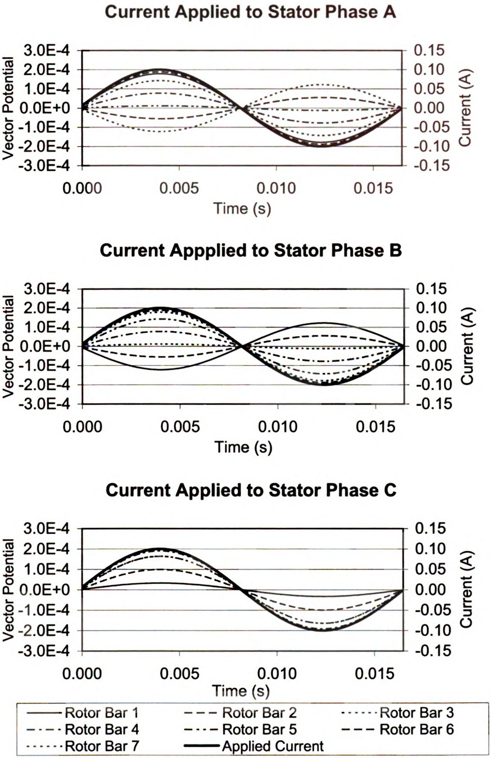

Figure 5.3. Outer rotor magnetic vector potentials (Wb/m) measured when current was applied to one stator phase.

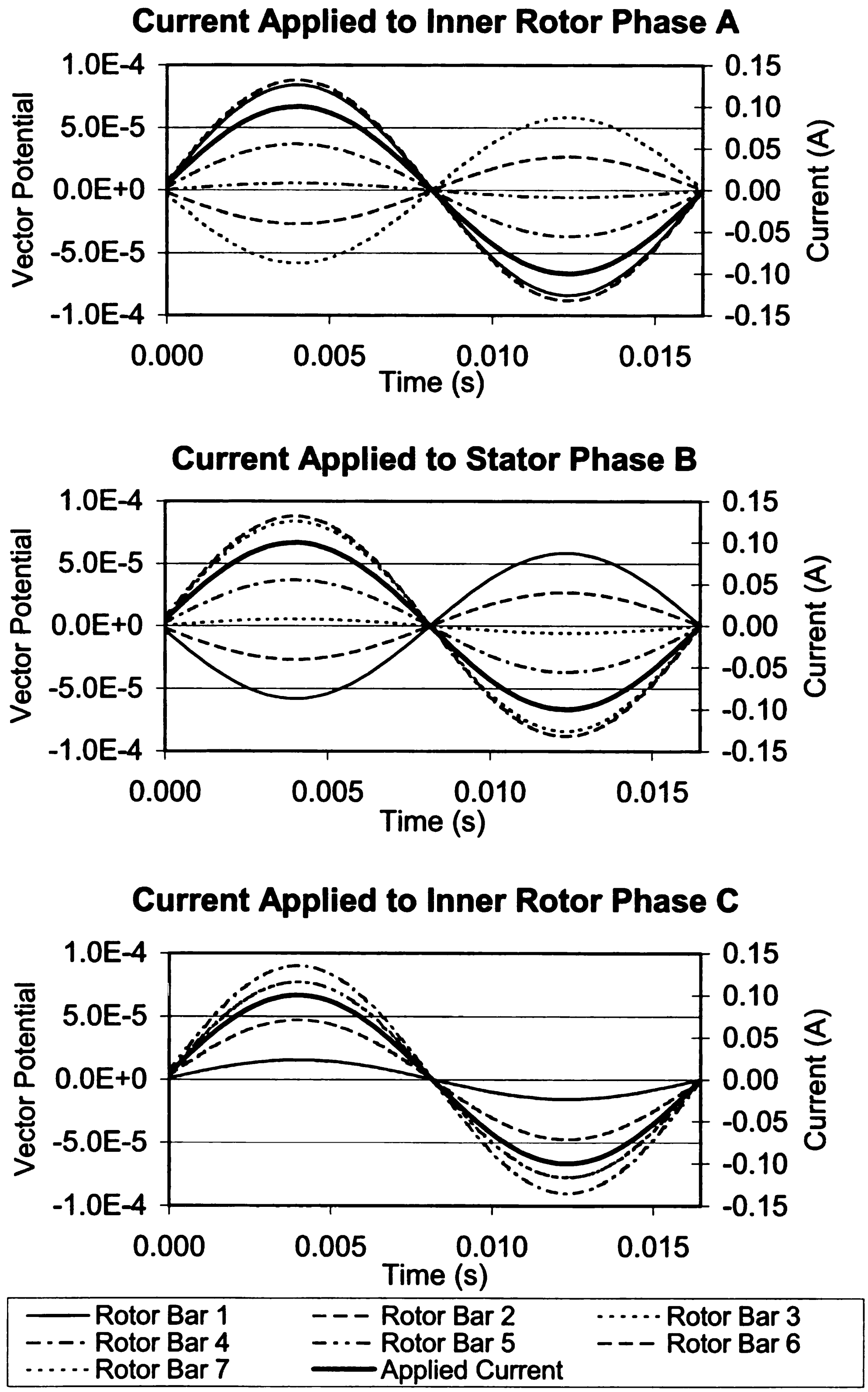

Figure 5.4. Outer rotor magnetic vector potentials (Wb/m) measured when current was applied to one inner rotor phase.

Rotor Region	SA	SB	SC	IRA	IRB	IRC
	Winding					
A	-67.1	-456.5	-456.7	-28.1	-215.0	-217.1
B	311.8	-459.1	-442.5	142.6	-221.1	-205.8
C	446.8	-451.2	-185.3	206.9	-213.9	-85.9
D	451.2	-446.8	185.3	213.9	-206.9	85.9
E	459.2	-311.8	442.5	221.1	-142.5	205.8
F	456.5	67.1	456.8	215.1	28.1	217.1
G	387.3	387.3	449.4	175.2	175.2	211.2

Table 5.13. Mutual inductance (μH) between the stator or inner rotor and the outer rotor regions.

regions can be found by dividing the magnetic flux in the region by the current applied to the stator or inner rotor as was described in equation (3.44). Table 5.13 contains the inductances found by applying this method. It is only necessary to calculate the inductance in one direction due to the linearity of the medium.

The mutual inductance between the stator and the outer rotor loops should be reduced to single value. This can be done by finding the magnitude of the stator to outer rotor mutual inductances curves formed by the inductances in Table 5.13. The magnitude can be found by dividing the inductances in the table by the sine of the angle between each rotor region and the sourced stator winding. Since the inductances don't have a perfect sinusoidal distribution, only those closest to the sourced coil will be used to find the average inductance. The resulting sine waves can be seen in Figure 5.5. After the magnitude is found for each mutual inductance the overall mutual inductance between the stator and outer rotor can be found by averaging the three resultant values.

$$L_{sor} = 829.7\mu H \tag{5.13}$$

The mutual inductance between the inner rotor and the outer loops can be found

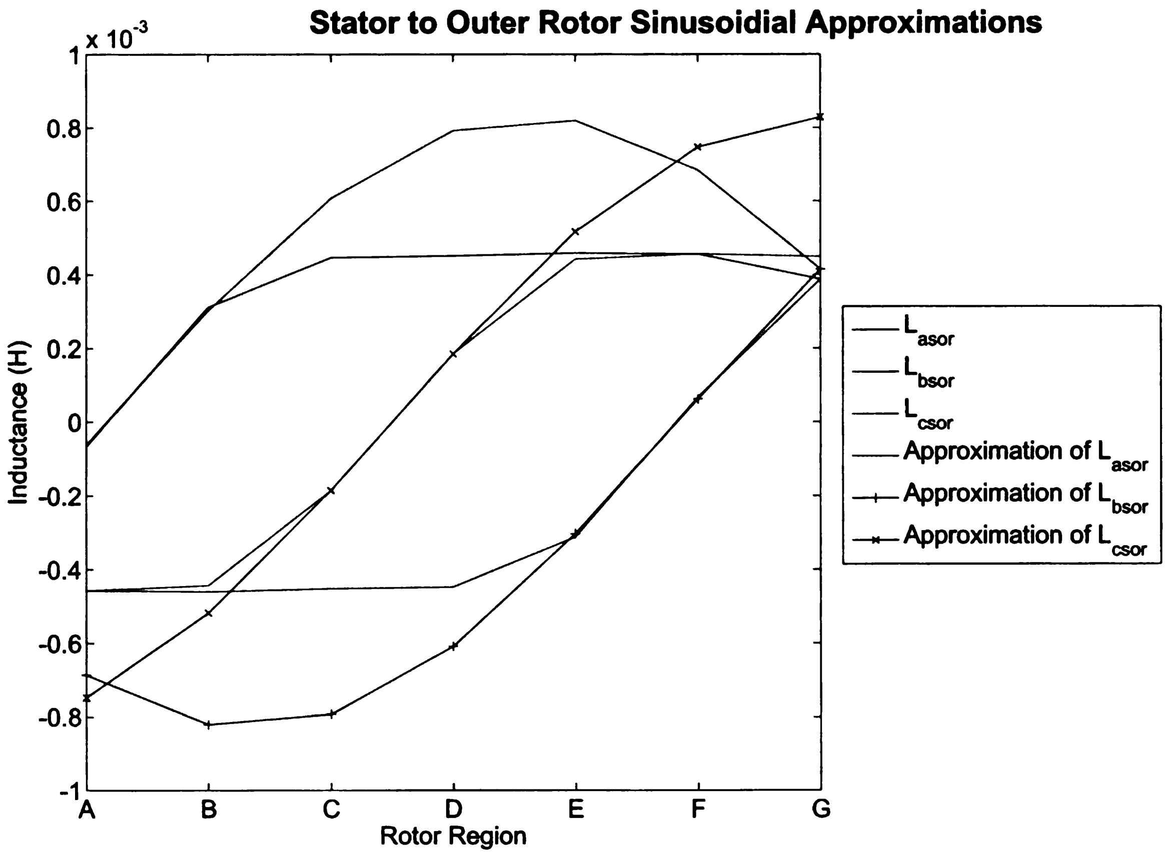

Figure 5.5. Stator to Outer Rotor Inductances

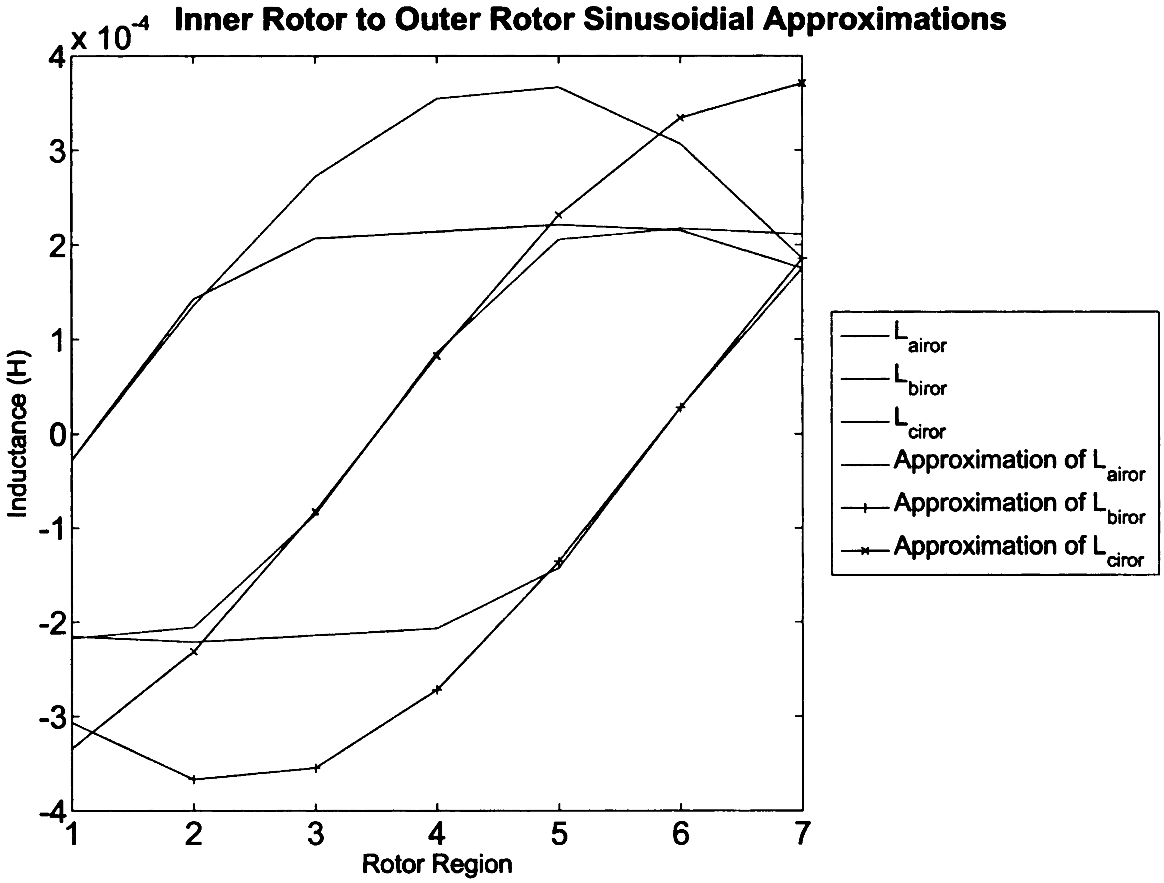

Figure 5.6. Inner Rotor to Outer Rotor Inductances

using the same method as was used to find the mutual inductance between the stator and the outer loops. Figure 5.6 shows the resulting sine waves.

$$L_{iror} = 371\mu H \tag{5.14}$$

CHAPTER 6

Model Development

6.1 Introduction

To create a model of the EVT, two sets of information are important: the frequencies of the currents and voltages throughout the machine and the voltage equations. With an understanding of both of these concepts it is possible to find the power distribution throughout the EVT. In this chapter these concepts will be developed. This information will then be used to develop the power flow throughout the EVT resulting in a model of the EVT.

6.2 Frequency Equations

In a traditional induction machine, the mechanical speed of the device can be controlled by the frequency of the currents applied to the stator. The EVT can be looked at as two separate induction machines with two controlled frequencies, ω_{ir} and ω_s, and two desired mechanical speeds, ω_{m1} and ω_{m2}. To control the speeds in the EVT, the frequencies throughout the machine should be established with respect to the controlled frequencies and the desired speed.

To begin, the stator and outer rotor relationships will be developed. The stator and outer rotor behave like the traditional stator and rotor in an induction machine. The frequency of the magnetic field in the outer airgap will be the same as the controlled frequency of the voltages in the stator. Since it has been established that the frequencies in both airgaps of the EVT must be the same, the frequency in the airgaps will be referred to as ω_f as seen in Figure 6.1.

$$p\omega_f = \omega_s \tag{6.1}$$

In a traditional induction machine the frequencies of the voltages in the rotor will be the difference between the frequency of the field in the gap and the mechanical speed of the rotor. The same relationship holds true for the stator and outer rotor of the EVT.

$$\omega_{or} = p(\omega_f - \omega_{m2}) = \omega_s - p\omega_{m2} \tag{6.2}$$

The slip is defined as the ratio of the difference between the frequency of the magnetic field in the airgap and the mechanical speed of the rotor divided by the frequency of the field in the gap. The slip between the outer rotor and the stator of the EVT will be the same as it was for an induction machine.

$$s_{outer} = \frac{\omega_{or}}{p\omega_f} = \frac{\omega_s - p\omega_{m2}}{\omega_s} \tag{6.3}$$

Now that the frequencies associated with the outer airgap have been established, the frequencies associated with the inner airgap can be established. The inner airgap can be viewed such that the inner rotor would act like a traditional stator and the outer rotor would, as it was in the case of the outer airgap, act like the rotor of a traditional induction machine. There is one noticeable difference. As opposed to the stator in a traditional induction machine which is stationary, the inner rotor is spinning at a mechanical speed ω_{m1}, in units of radians per second. With this in

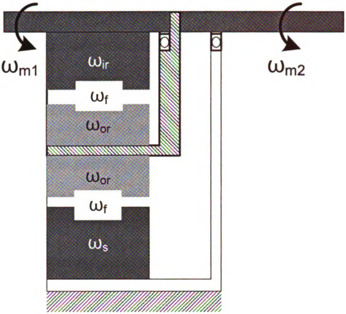

Figure 6.1. EVT frequency definitions

mind, the frequency of the magnetic field in the inner airgap can be described in terms of the mechanical speed of the inner rotor and the applied frequencies of the voltages found in the inner rotor.

$$p\omega_f = \omega_{ir} + p\omega_{m1} \tag{6.4}$$

It would follow that the frequencies of the voltages found in the inner rotor would be

$$\omega_{ir} = p(\omega_f - \omega_{m1}). \tag{6.5}$$

In the EVT the frequencies for the magnetic field in the inner and outer gaps must be equal and therefore, the rotor frequency must be the same for both the inner and outer airgaps. As such, the frequency of the currents and voltages in the outer rotor can be described in terms of the mechanical speeds of the rotors and the applied frequency of the voltages in the inner rotor.

$$\omega_{or} = \omega_{ir} - p(\omega_{m2} - \omega_{m1}) \tag{6.6}$$

The slip is again described as the ratio of the difference between the frequency of the field in the gap and the mechanical speed of the outer rotor. Since the inner rotor is spinning at a mechanical speed, ω_{m1}, the slip in the inner gap can be described as

$$s_{inner} = \frac{\omega_{or}}{p\omega_f} = \frac{\omega_{ir} - p(\omega_{m2} - \omega_{m1})}{\omega_{ir} + p\omega_{m1}}. \tag{6.7}$$

6.3 Voltage Equations

The voltage in the stator will consist of three parts. The first part will be due to the currents flowing in the stator and the impedance of the stator windings. The second component is due to the impedance caused by the mutual inductance between the stator windings and the inner rotor windings. The final component is again due to impedance caused by mutual inductance. This time the mutual inductance is found between the stator and the outer rotor. If these components are combined, an equation for the stator voltage will be created.

$$\mathbf{V_s} = (\mathbf{R_s} + \mathbf{X_s})\mathbf{i_s} + \mathbf{X_{irs}}\mathbf{i_{ir}} + \mathbf{X_{ors}}\mathbf{i_{or}} \tag{6.8}$$

The voltages in the inner rotor will have the same basic structure. There will be one component due to the impedance of the rotor and two components due to the impedance caused by the mutual inductance with the other two machine components.

$$\mathbf{V_{ir}} = (\mathbf{R_{ir}} + \mathbf{X_{ir}})\mathbf{i_{ir}} + \mathbf{X_{sir}}\mathbf{i_s} + \mathbf{X_{orir}}\mathbf{i_{or}} \tag{6.9}$$

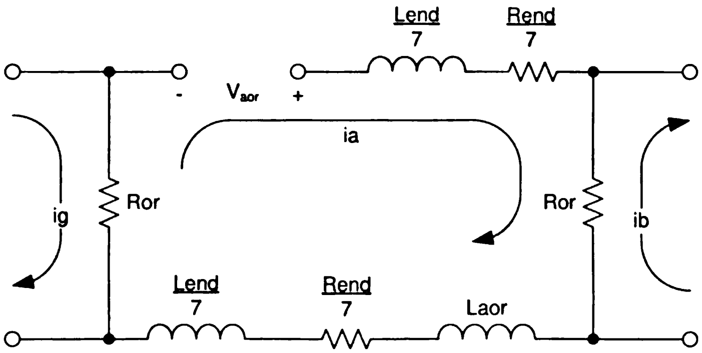

Figure 6.2. Outer rotor equivalent circuit for outer rotor bars 1 and 2

The outer rotor is a bit more complex. Since the outer rotor consists of rotor bars and not windings, we need to account for the rotor bar ends not present in the stator and inner rotor.

Figure 6.2 shows the equivalent circuit for the inner rotor bars one and two ignoring, for now, the mutual inductances. The circuit can be solved for the current in the outer rotor loop a composed of the rotor bar ends and rotor bars one and two. Using Kirchoff's voltage law, the voltage in rotor loop a, V_{aor}, would be as follows.

$$V_{aor} = (X_{aor} + \frac{2}{7}X_{end} + \frac{2}{7}R_{end} + 2R_{or})i_a - R_{or}i_b - R_{or}i_g \tag{6.10}$$

Equations of the form of equation (6.10) can be applied to any of the loops enclosed by a pair of adjacent rotor bars. If the mutual inductances are no longer ignored, equation (6.10) can then be written in vector notation

$$\begin{aligned}\mathbf{V_{or}} = {} & (\mathbf{X_{or}} + 2R_{or}\mathbf{I} + \frac{2}{7}R_{end}\mathbf{I} + \frac{2}{7}X_{end}\mathbf{I})\mathbf{i_{or}} \\ & -R_{or}\mathbf{I}(\mathbf{i_{or}^{+1}} + \mathbf{i_{or}^{-1}}) + \mathbf{X_{sor}}\mathbf{i_s} + \mathbf{X_{iror}}\mathbf{i_{ir}}\end{aligned} \tag{6.11}$$

Equation (6.11) can be modified to fit the form of equations (6.8) and (6.9).

$$\mathbf{V_{or}} = (2\mathbf{R_{or}} - \mathbf{R_{or}^{+1}} - \mathbf{R_{or}^{-1}} + \frac{2}{7}\mathbf{R_{end}} + \mathbf{X_{or}} + \frac{2}{7}\mathbf{X_{end}})\mathbf{i_{or}} + \mathbf{X_{sor}}\mathbf{i_s} + \mathbf{X_{iror}}\mathbf{i_{ir}} \tag{6.12}$$

6.4 EVT Model

Everything needed to fully model the EVT is now known. The equations developed in Section 6.3 can now be reevaluated taking into account the frequency equations established in Section 6.2. The voltage equations will be established with the frequencies described in terms of the controllable values, ω_{ir} and ω_s, and the desired mechanical speeds, ω_{m1} and ω_{m2}. Equations (6.13) through (6.16) represent the EVT model.

$$\mathbf{V_s} = (\mathbf{R_s} + j\omega_s\mathbf{L_s})\mathbf{i_s} + j\omega_{ir}\mathbf{L_{irs}}\mathbf{i_{ir}} + j\omega_{or}\mathbf{L_{ors}}\mathbf{i_{or}} \tag{6.13}$$

$$\mathbf{V_{ir}} = (\mathbf{R_{ir}} + j\omega_{ir}\mathbf{L_{ir}})\mathbf{i_{ir}} + j\omega_s\mathbf{L_{sir}}\mathbf{i_s} + j\omega_{or}\mathbf{L_{orir}}\mathbf{i_{or}} \tag{6.14}$$

$$\begin{aligned}\mathbf{V_{or}} = (2\mathbf{R_{or}} - \mathbf{R_{or}^{+1}} - \mathbf{R_{or}^{-1}} + \frac{2}{7}\mathbf{R_{end}} + j\omega_{or}\mathbf{L_{or}} \\ + \frac{2}{7}j\omega_{or}\mathbf{L_{end}})\mathbf{i_{or}} + j\omega_s\mathbf{L_{sor}}\mathbf{i_s} + j\omega_{ir}\mathbf{L_{iror}}\mathbf{i_{ir}}\end{aligned} \tag{6.15}$$

where,

$$\omega_{or} = \omega_s - p\omega_{m2} = \omega_{ir} - p(\omega_{m2} - \omega_{m1}). \tag{6.16}$$

6.5 Torque Equations

The energy stored in the coupling field of a linear rotational electromagnetic system with J electrical inputs can be expressed as in equation (6.17).

$$W_f(i_1, ..., i_j, \theta) = \frac{1}{2}\sum_{p=1}^{J}\sum_{q=1}^{J} L_{pq} i_p i_q \tag{6.17}$$

In the case of the EVT, there are three electrical inputs, the stator, the inner rotor and the outer rotor. The EVT has three coupling fields: one between the stator and outer rotor, one between the inner rotor and outer rotor and one between the stator and outer rotor. The coupling field between the inner rotor and outer rotor will be referred to as W_{g1}, the field between the stator and outer rotor as W_{g2}, and finally the field between the stator and inner rotor as W_{rs}. Equation (6.17) can be solved for the coupling field between the inner and outer rotors.

$$W_{g1} = \frac{1}{2}(\mathbf{i}_{ir})^T(\mathbf{L}_{ir})\mathbf{i}_{ir} + (\mathbf{i}_{ir})^T\mathbf{L}_{iror}\mathbf{i}_{or} + \frac{1}{2}(\mathbf{i}_{or})^T(\mathbf{L}_{or})\mathbf{i}_{or} \tag{6.18}$$

The equations for the other two torque components, T_{g2} and T_{rs}, would be of the same form as equation (6.18).

The electromagnetic torque of a rotational system at the kth mechanical input can be described as in equation (6.19).

$$T_{ek}(i_j, \theta_r) = \left(\frac{P}{2}\right)\frac{\partial W_c(i_j, \theta_r)}{\partial \theta_r} \tag{6.19}$$

Since it was assumed that the machine is linear, the coupling field energy is equal to the coenergy, $W_f = W_c$. Equations of the type of equation (6.19) can now be used to find the torque. In order to find the torque, W_c can be replaced with equation (6.17). In equation (6.18) only the mutual inductances between the inner and outer rotors are functions of θ_{iror}. Therefore, to solve for the torque, the self inductance components of equation (6.18) can be ignored.

$$T_{g1} = \left(\frac{P}{2}\right)(\mathbf{i}_{ir})^T[\mathbf{L}_{iror}]\mathbf{i}_{or} \tag{6.20}$$

The electromagnetic torque for the coupling fields W_{g2} and W_{rs} would have similar forms to that of equation (6.20). Solving for the partial derivative the torques would become

$$T_{g1} = -\left(\frac{P}{2}\right)\hat{L}_{iror}\mathbf{i}_{ir}\{[-cos(\epsilon_{iror})sin(\theta_{iror}) - sin\epsilon_{iror})cos(\theta_{iror})]\mathbf{i}_{or}\} \qquad (6.21)$$

$$T_{g2} = -\left(\frac{P}{2}\right)\hat{L}_{sor}\mathbf{i}_{s}\{[-cos(\epsilon_{sor})sin(\theta_{sor}) - sin(\epsilon_{sor})cos(\theta_{sor})]\mathbf{i}_{or}\} \qquad (6.22)$$

$$T_{rs} = -\left(\frac{P}{2}\right)\hat{L}_{sir}\mathbf{i}_{s}\{[-cos(\epsilon_{sir})sin(\theta_{sir}) - sin(\epsilon_{sir})cos(\theta_{sir})]\mathbf{i}_{ir}\} \qquad (6.23)$$

where ϵ is the relative angular position defined as

$$\epsilon_{sir} = \begin{pmatrix} 0 & \frac{2\pi}{3} & -\frac{2\pi}{3} \\ -\frac{2\pi}{3} & 0 & \frac{2\pi}{3} \\ \frac{2\pi}{3} & -\frac{2\pi}{3} & 0 \end{pmatrix}$$

$$\epsilon_{sor} = \begin{pmatrix} 0 & \frac{2\pi}{7} & \frac{4\pi}{7} & \frac{6\pi}{7} & -\frac{6\pi}{7} & -\frac{4\pi}{7} & -\frac{2\pi}{7} \\ -\frac{2\pi}{3} & -\frac{8\pi}{21} & -\frac{2\pi}{21} & \frac{4\pi}{21} & -\frac{32\pi}{21} & -\frac{26\pi}{21} & -\frac{20\pi}{21} \\ \frac{2\pi}{3} & \frac{20\pi}{21} & \frac{26\pi}{21} & \frac{32\pi}{21} & -\frac{4\pi}{21} & \frac{2\pi}{21} & \frac{8\pi}{21} \end{pmatrix}$$

$$\epsilon_{iror} = \begin{pmatrix} 0 & \frac{2\pi}{7} & \frac{4\pi}{7} & \frac{6\pi}{7} & -\frac{6\pi}{7} & -\frac{4\pi}{7} & -\frac{2\pi}{7} \\ -\frac{2\pi}{3} & -\frac{8\pi}{21} & -\frac{2\pi}{21} & \frac{4\pi}{21} & -\frac{32\pi}{21} & -\frac{26\pi}{21} & -\frac{20\pi}{21} \\ \frac{2\pi}{3} & \frac{20\pi}{21} & \frac{26\pi}{21} & \frac{32\pi}{21} & -\frac{4\pi}{21} & \frac{2\pi}{21} & \frac{8\pi}{21} \end{pmatrix}$$

CHAPTER 7

Model Validation

To prove that the model developed actually represents a true machine, it must be validated. Since an actual machine is not available the model will have to be tested against a set of expected results. This section details a series of tests and their results to verify the accuracy of the model. For all of the following tests, the machine variables developed using the FEA process for the four pole machine presented earlier will be used.

7.1 Test 1 - Stator to Outer Rotor Linkage

This test treats the stator as a traditional stator and the outer rotor as a traditional rotor. The inner rotor will be made an open circuit. The inner rotor will also be held stationary for this test. This test shows the ability to pass energy from the stator to the outer rotor.

7.1.1 Setup

To simulate this situation, the stator voltage will be set to $V_s = 120V$. Both the inner and outer rotor applied voltages will be set to 0 V, $V_{ir} = V_{or} = 0V$. A large resistance, 20 kΩ, will be added in series to each inner rotor phase to simulate an open circuit. To simulate a stationary inner rotor, the speed of machine 1 will be set to 0 rpm, $\omega_{m1} = 0rpm$. To create a torque, a slip needs to be introduced between the stator and outer rotor, $\omega_{slip} = 30rpm$. In order to have a synchronous speed of 1800 rpm, the outer rotor speed will be set to 1785 rpm, $\omega_{m2} = 1785rpm$.

7.1.2 Results

In this case the stator currents settle out to sinusoidal signals at a frequency of 60 Hz. Since the inner rotor is an open circuit and stationary, the inner rotor currents were also at 60 Hz but the amplitude was relatively small in comparison to the stator and outer rotor currents. The inner rotor currents were 90 degrees out of phase with respect to the stator currents. The outer rotor currents settled out to be sinusoidal at 0.5 Hz.

There is torque between all three parts of the machine. The torque is positive in the outer airgap and settles out to approximately 0.14 Nm. The inner airgap torque is negative but is negligible in comparison to the outer airgap torque. There is a relatively small torque between the inner rotor and stator in comparison to the outer airgap torque.

7.2 Test 2 - Inner Rotor to Outer Rotor Linkage

This test treats the inner rotor as a traditional stator and the outer rotor as a traditional rotor. The inner rotor will be held stationary for this test. The stator will be made to act as an open circuit for this test. This tests the ability to pass energy from the inner rotor to the outer rotor.

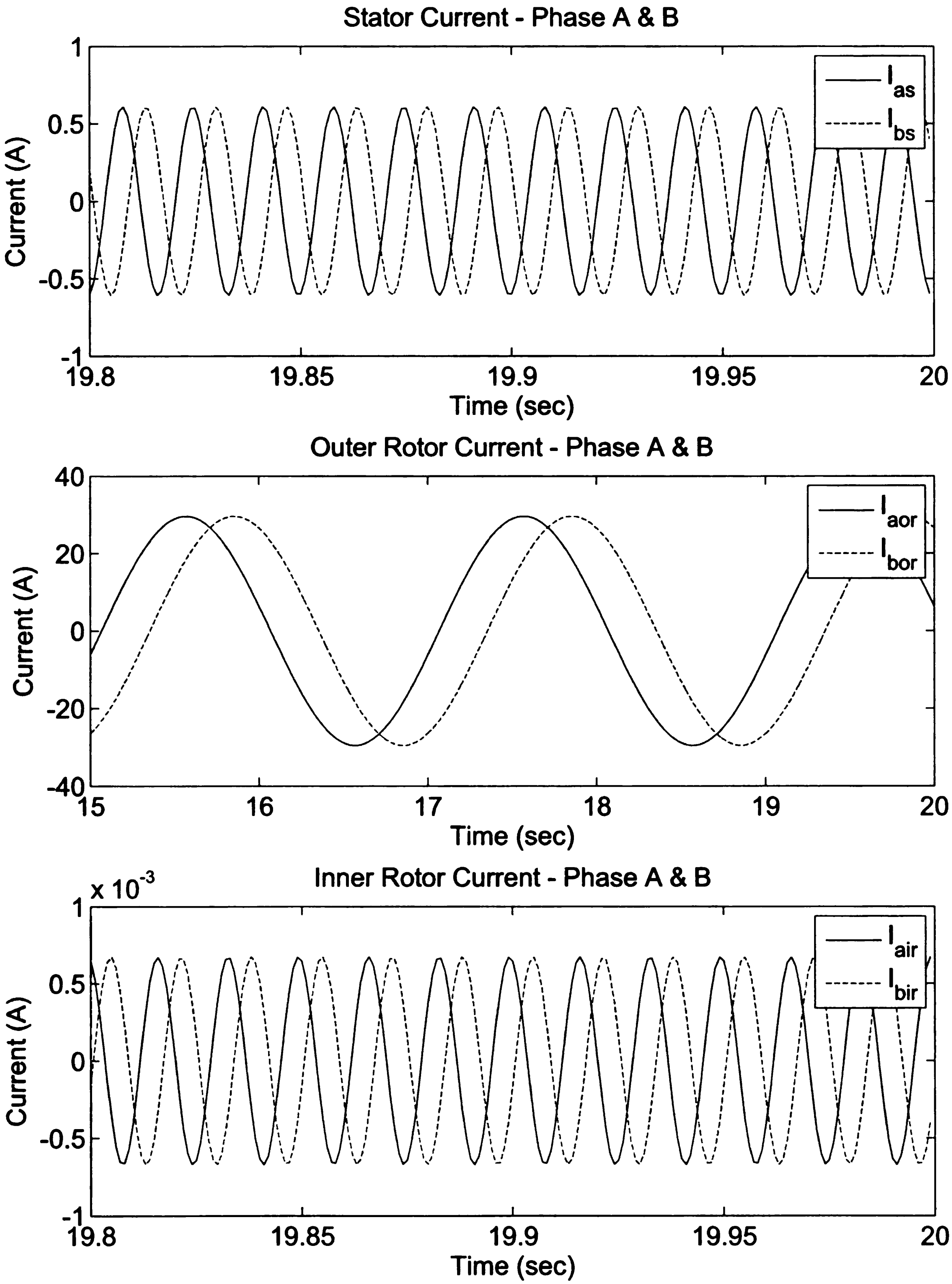

Figure 7.1. Machine currents (A) measured during Test 1.

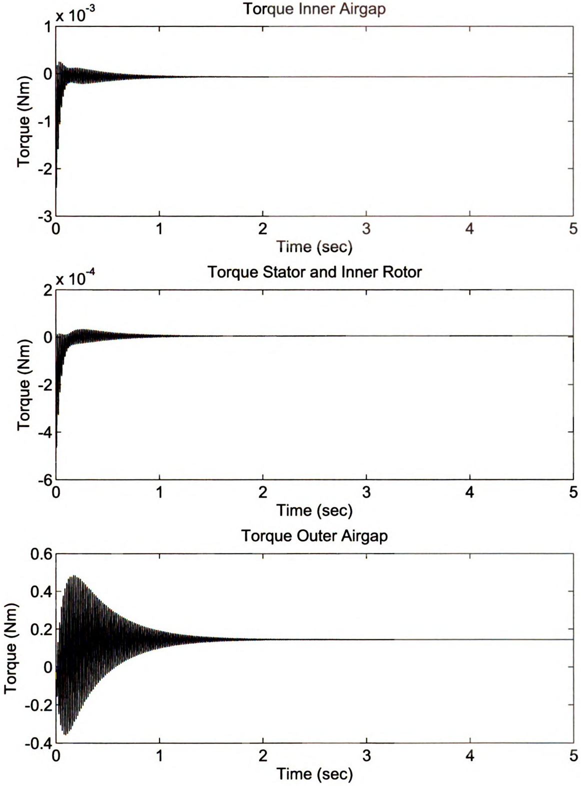

Figure 7.2. Torque between the machine parts measured during Test 1.

7.2.1 Setup

For the validation of the linkage between the inner and outer rotors, the inner rotor voltage will be set to 120V, $V_{ir} = 120V$. The stator and outer rotor will both have no applied voltage, $V_s = V_{or} = 0V$. The stator will have large series resistances, 20 kΩ, added to each phase to simulate an open circuit. The inner rotor will again not be allowed to rotate $\omega_{m1} = 0rpm$. The slip frequency will again be set to 30 rpm, $\omega_{slip} = 30rpm$ and the outer rotor will be allowed to spin at 1785 rpm, $\omega_{m2} = 1785rpm$.

7.2.2 Results

The stator currents are as they were expected to be, sinusoidal signals at 60 Hz with a relatively low amplitude. The inner rotor currents are also 60 Hz sine waves but they lead the stator currents by 90 degrees. The outer rotor currents are sinusoidal and settled out to a frequency of 0.5 Hz.

There is torque between all three parts of the machine. The torque in the outer airgap and the torque between the stator and in inner rotor are both negligible. The torque is positive in the inner airgap with a steady state value of 0.13 Nm. These results are all as expected.

7.3 Test 3 - Stator to Inner Rotor Linkage

The purpose of Test 3 is to check to make sure that energy is being transfered from the stator to the inner rotor. The outer rotor will be held stationary for this test. The stator will be treated as a traditional stator and the inner rotor a traditional rotor.

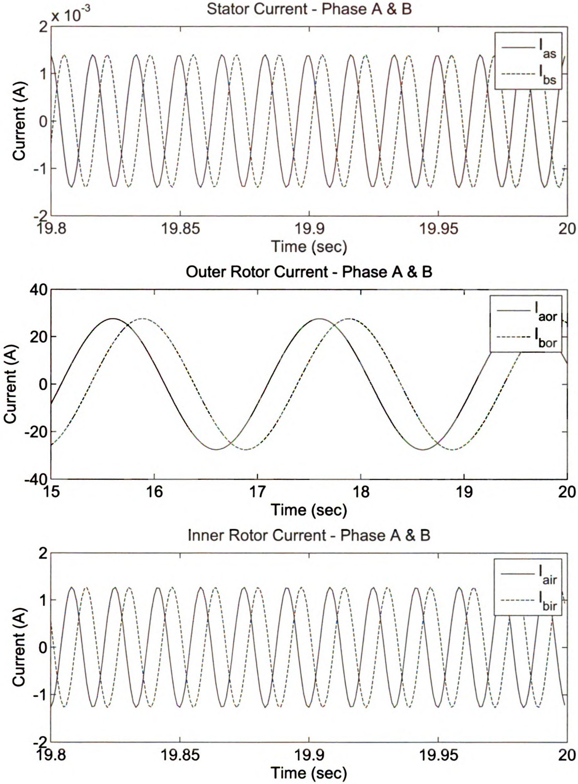

Figure 7.3. Machine currents (A) measured during Test 2.

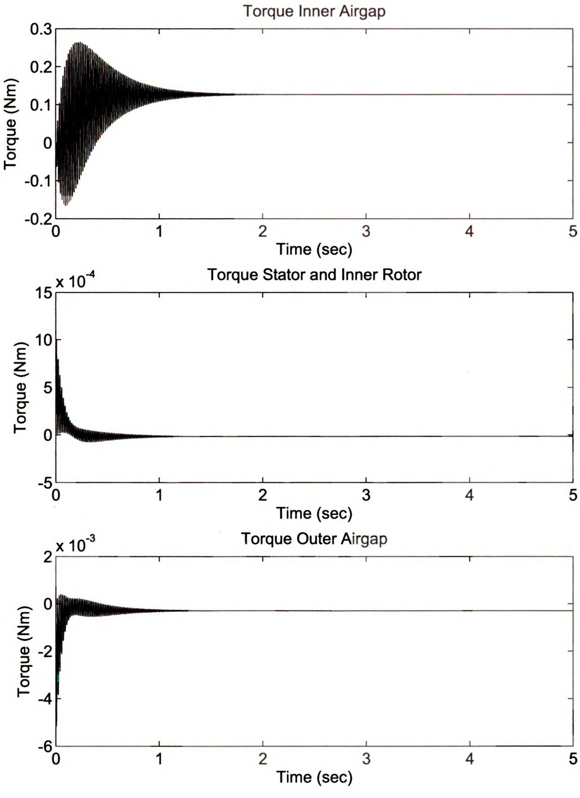

Figure 7.4. Torque between the machine parts measured during Test 2.

7.3.1 Setup

To validate the transfer of power from the stator to the inner rotor the stator voltage will be set to 120V, $V_s = 120$. The outer rotor will have a relatively large load applied to it, 3 Ω. This value is much smaller than the resistance applied in the other tests. This was done to decrease the time to solve using the ordinary differential equation solver. The inner rotor will be made a short circuit by setting the applied voltage to 0V, $V_{ir} = 0$. The outer rotor will not be allowed to rotate $\omega_{m2} = 0rpm$. The inner rotor will be allowed to spin at 1795 rpm $\omega_{m1} = 1795rpm$. The slip will be set to 10, $\omega_{slip} = 10$. The slip value used for this test was set to a value less than the slip used in the previous tests because the torque speed characteristics are slightly different when the EVT is configured as it is in this test. Since this is not a normal operating point, the model will have to be varied slightly. The frequency in the stator will be set as

$$\omega_s = p\omega_{m1} + \omega_{slip} \tag{7.1}$$

7.3.2 Results

The stator currents are sinusoidal with a frequency of 60 Hz. The outer rotor currents are also sinusoidal at 60 Hz but they are 90 degrees out of phase with the rotor currents. The inner rotor currents are sinusoidal at a frequency of 0.1667 Hz.

The torque developed in the inner and outer airgap was extremely small. The torque developed between the stator and inner rotor was larger than that developed in either airgap but was still relatively small, 0.000942 Nm. This was as expected. Some torque was developed between the stator and inner rotor displaying that there is an interaction developed. The effect, in comparison to the torques developed in Tests 1 and 2, is relatively small.

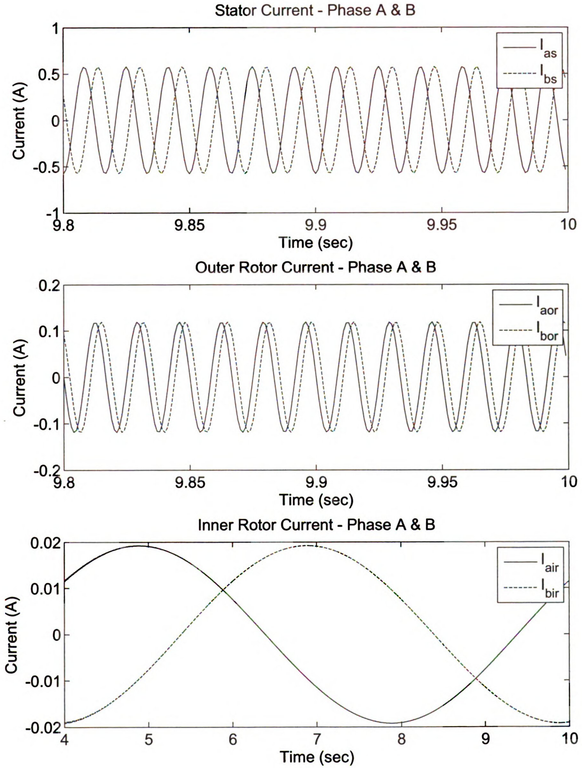

Figure 7.5. Machine currents (A) measured during Test 3.

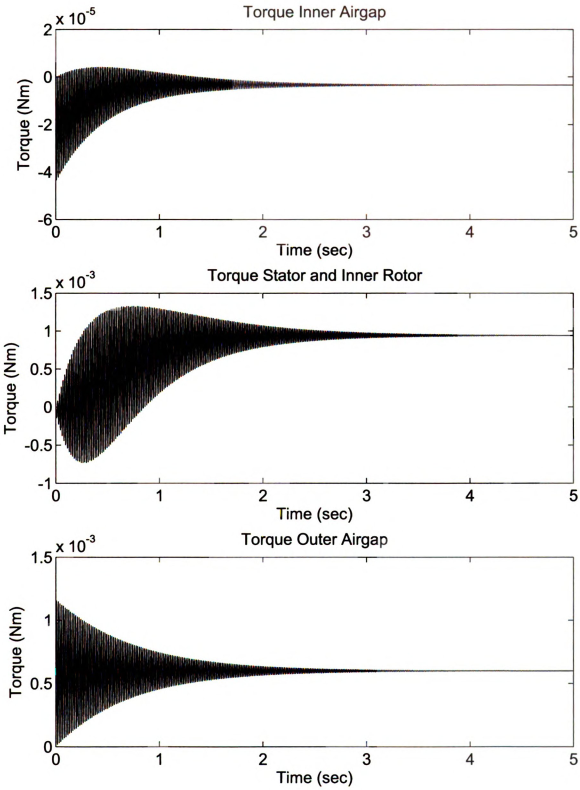

Figure 7.6. Torque between the machine parts measured during Test 3.

7.4 Test 4 - Stator to Outer Rotor High Slip

The purpose of this test is to show the relationship of slip and torque between the stator and the outer rotor. In this case, much will be the same as Test 1. The difference being that the slip will be increased. The increased slip should show an increased torque between the stator and outer rotor then that which was measured in Test 1.

7.4.1 Setup

For this test, the stator voltage will be set to $V_s = 120V$. Both the inner and outer rotor applied voltages will be set to zero, $V_{ir} = V_{or} = 0V$. To simulate an open inner rotor, a large resistance, 20 kΩ, will be added in series with each inner rotor phase. To simulate a stationary inner rotor, the speed of machine 1 will be set to 0 rpm, $\omega_{m1} = 0rpm$. To create a greater torque than in Test 1 a greater slip needs to be introduced between the stator and outer rotor. The slip will be set to twice what it was in Test 1, $\omega_{slip} = 60rpm$. To have a synchronous speed of 1800 rpm we will set the outer rotor speed to 1770 rpm, $\omega_{m2} = 1770rpm$.

7.4.2 Results

In this case, the stator currents settles out to sinusoidal signals at a frequency of 60 Hz just as was in Test 1. The inner rotor currents were also at 60 Hz but the magnitude of the currents was much lower then the stator and outer rotor currents. The outer rotor currents settled out to be sinusoidal at 1 Hz with an amplitude of about twice that of the currents in Test 1.

The torque between the stator and inner rotor and the torque in the inner airgap are both negligible. The torque is positive in the outer airgap, 0.2754 Nm, and larger then the torque found in Test 1 as was expected.

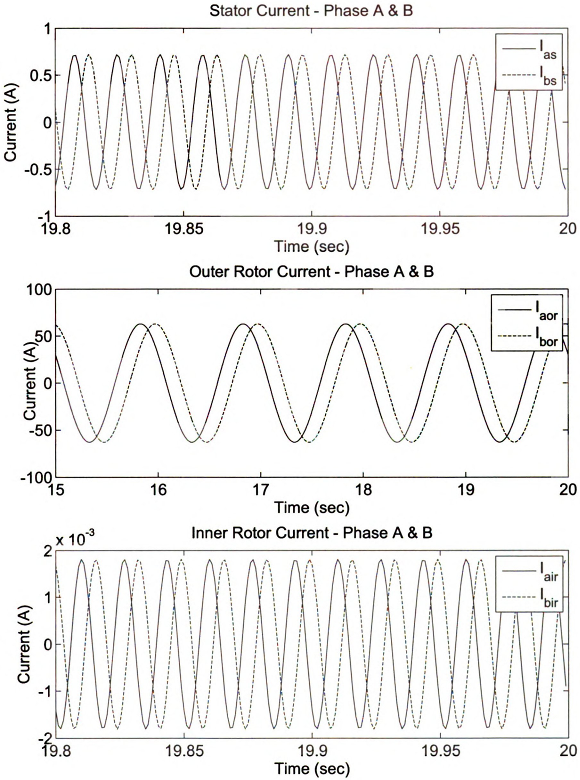

Figure 7.7. Machine currents (A) measured during Test 4.

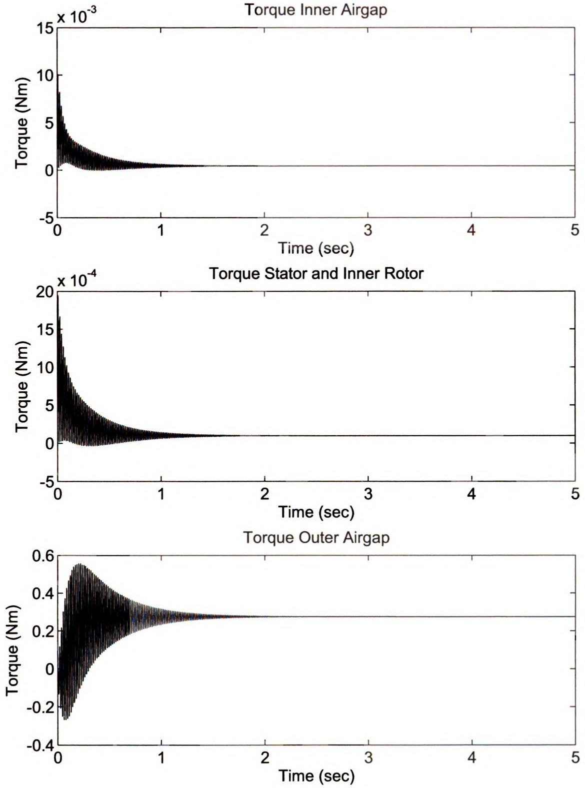

Figure 7.8. Torque between the machine parts measured during Test 4.

7.5 Test 5 - Inner Rotor to Outer Rotor High Slip

This test is meant to show that the torque between the inner and outer rotors varies as the slip between those parts varies. This test will be a repeat of Test 2 with an increased slip.

7.5.1 Setup

To show that the torque between the inner and outer rotors varies with the slip between them, we will use many of the same values as we used in Test 2. Again, the inner rotor voltage will be set to 120V, $V_{ir} = 120V$. The stator will again have series resistances of 20 kΩ added to each phase. The inner rotor will again, not be allowed to rotate, $\omega_{m1} = 0rpm$. The difference between this test and Test 2 will be that the slip frequency will be set to 60 rpm, $\omega_{slip} = 60rpm$. Therefore, to maintain a synchronous speed of 1800 rpm the outer rotor will be allowed to spin at 1770 rpm, $\omega_{m2} = 1770rpm$.

7.5.2 Results

The inner rotor currents are as expected: sinusoidal signals with a frequency at 60 Hz. The stator currents are also 60 Hz sine waves with an amplitude much less than the inner and outer rotor currents. The outer rotor currents settle out to be sinusoidal with a frequency of 1 Hz with an amplitude larger than that found in Test 2.

The torque in the inner airgap is positive with an amplitude of approximately 0.19 Nm. This torque value is greater than the torque found in Test 2. The other torque values in the machine are both negligible. These results are all as expected.

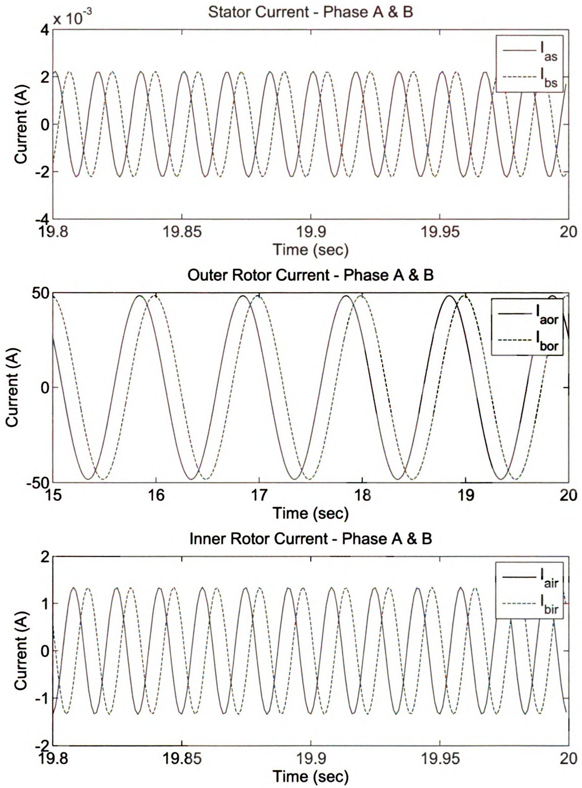

Figure 7.9. Machine currents (A) measured during Test 5.

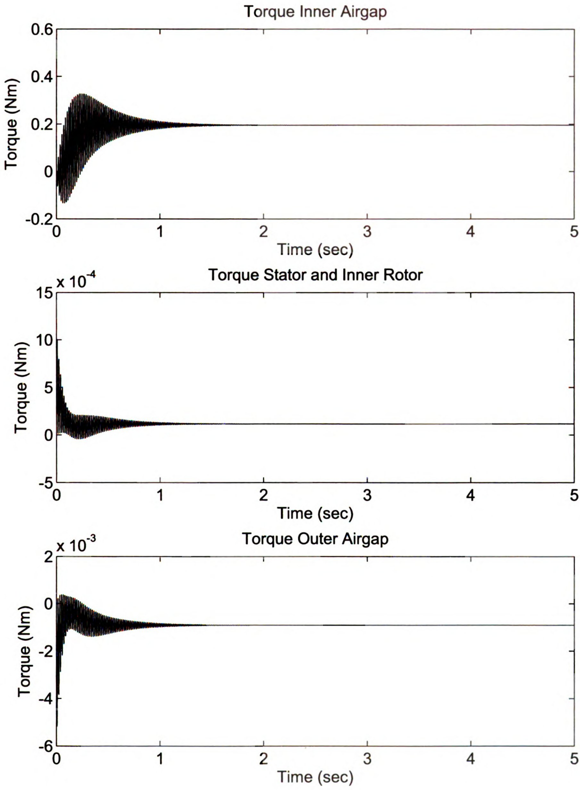

Figure 7.10. Torque between the machine parts measured during Test 5.

7.6 Test 6 - Stator to Inner Rotor High Slip

To confirm that the torque between the stator and inner rotor varies with the slip of those two components, Test 3 will be rerun this time with a slip that is greater than that in Test 3. When complete, the results of this test can be compared to the previous results to show the relationship of slip to torque between the stator and inner rotor.

7.6.1 Setup

To show that the torque between the stator and inner rotor varies with the slip between those components, all of the values used in Test 3 will again be used for this test except for the slip speed. The stator voltage will be set to 120V, $V_s = 120$. Both the inner and outer rotor applied voltages will be set to zero, $V_{ir} = V_{or} = 0$. The outer rotor will again be made an open circuit by applying a relatively large resistance, 3Ω. The outer rotor will not be allowed to rotate, $\omega_{m2} = 0rpm$. The inner rotor will be allowed to spin at 1785 rpm $\omega_{m1} = 1785rpm$. The slip will be set to 30 rpm, $\omega_{slip} = 30rpm$. The frequencies in the model will be modified as they were in Test 3.

7.6.2 Results

The stator currents are sinusoidal at 60 Hz as they were in Test 3. The outer rotor currents are also sinusoidal at 60 Hz but they lag the stator currents. The inner rotor currents are sinusoidal at 0.5 Hz as expected.

As was the case in Test 3, the torque developed in the inner and outer airgaps was relatively small in comparison to the torque between the stator and inner rotor. The torque developed between the stator and inner rotor was larger than that developed in either airgap but was still relatively small, 0.00126 Nm. This value is larger than

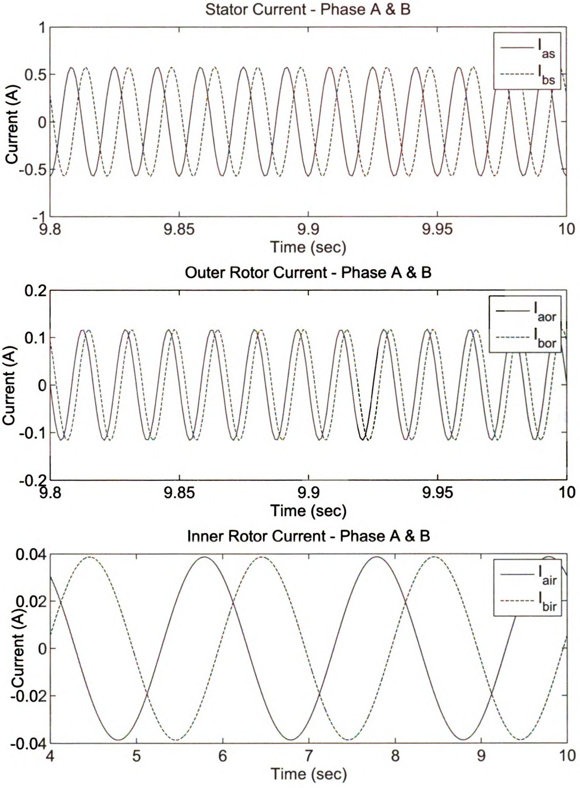

Figure 7.11. Machine currents (A) measured during Test 6.

that found in Test 3. This shows that near synchronous speed the torque between the stator and inner rotor will increase as the slip between those two components increase.

7.7 Test 7 - Both Rotors in Motion

The purpose of this test is to show that the relative motion of the inner rotor to outer rotor is what causes the torque to be transfered, not the absolute speed. To show this Test 2 will be repeated. This time, both rotors will be in motion.

7.7.1 Setup

All of the voltages used in Test 2 will be used for this test. The difference will be in the speeds. The outer rotor will be allowed to rotate at 2785 rpm, $\omega_{m2} = 2785rpm$. The inner rotor will be rotated at 1000 rpm, $\omega_{m1} = 1000rpm$. This will result in the same slip speed, $\omega_{slip} = 30$, as used in Test 2.

7.7.2 Results

The currents in the inner rotor are sinusoidal at 60 Hz. They have relatively the same magnitude and the same frequency as the inner rotor currents did in Test 2. The currents in the outer rotor are sinusoidal with a frequency of 0.5 Hz. They have relatively the same magnitude and frequency as the currents found in Test 2. The stator currents have a slightly higher magnitude as those in Test 2 but the frequency is now closer to 90 Hz. The magnitude of the stator currents is still much lower than the inner and outer rotor currents. The slightly higher currents in all of the components are due to the increased slip between the stator and inner rotor and the stator and outer rotor. The effect is negligible but should be noted.

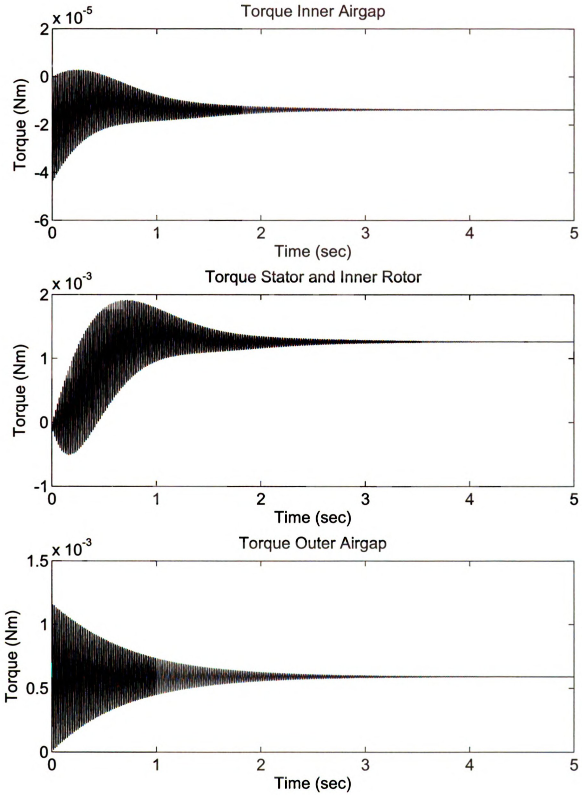

Figure 7.12. Torque between the machine parts measured during Test 6.

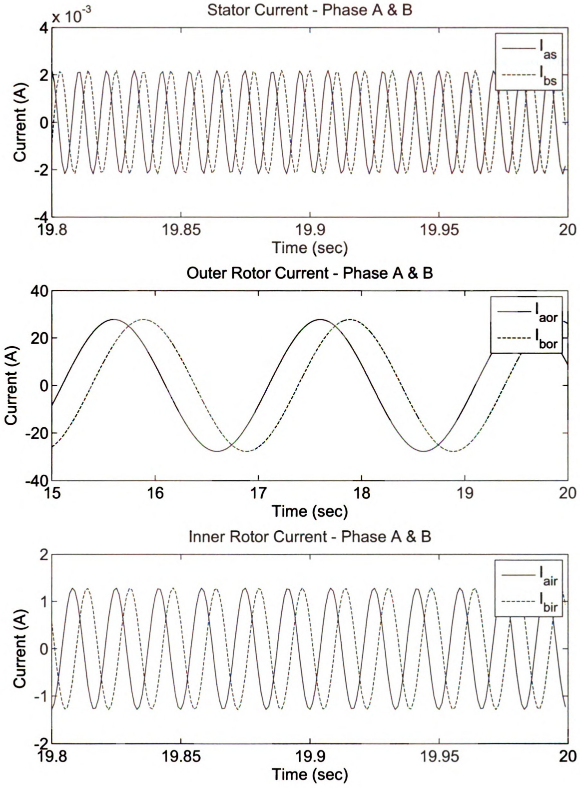

Figure 7.13. Machine currents (A) measured during Test 7.

The steady state torque in the inner airgap is positive and is relatively equivalent to the torque found in Test 2. The steady state torque in the outer airgap is also relatively the same value as found in Test 2. The torque between the stator and inner rotor is relatively close to what it was in Test 2. This is the expected result as the slip with respect to the stator has changed but the effect is negligible.

7.8 Test 8 - Stator Torque Speed Curve

For this test, the goal is to create the torque speed curve for the stator when the inner rotor is an open circuit. This test is different from the previous tests as it is not as much about verification of the model as about getting information from the model.

7.8.1 Setup

The voltage of the stator will be set to 120V, $V_s = 120V$. The inner and outer rotor applied voltages will be set to zero, $V_{ir} = V_{or} = 0$. Since we are looking for a torque speed curve the slip and supply frequencies will be modified directly. The stator frequency will be held constant at synchronous speed, $\omega_s = 2\pi 60$ rad/s. The slip frequency will be varied from 100 rpm to 3600 rpm, $\omega_{slip} = \frac{10\pi}{3}$ to $2\pi 60$. For this test, the inner rotor will be held stationary, $\omega_{m1} = 0$. The slip frequency will be applied directly to the outer rotor, $\omega_{or} = \omega_{slip}$. The inner rotor will be made an open circuit by applying a series resistance of 20 kΩ to each of the inner rotor phases.

The result will not be a true torque speed curve because the speed will be swept from zero to twice synchronous speed throughout the test. To get a true torque speed curve, the model would need to be allowed to hold at set speeds for a given time period in order to reach steady state. The torque speed curve from this test will only be useful to give basic characteristic data about the EVT.

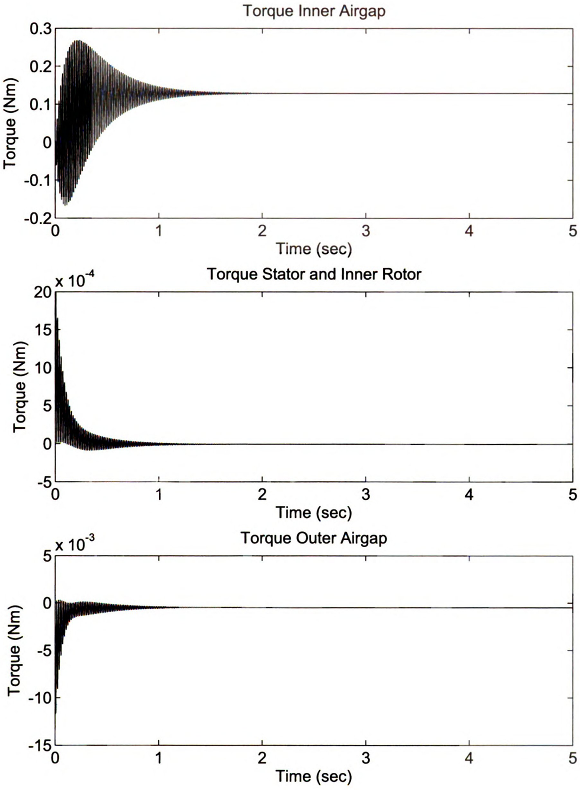

Figure 7.14. Torque between the machine parts measured during Test 7.

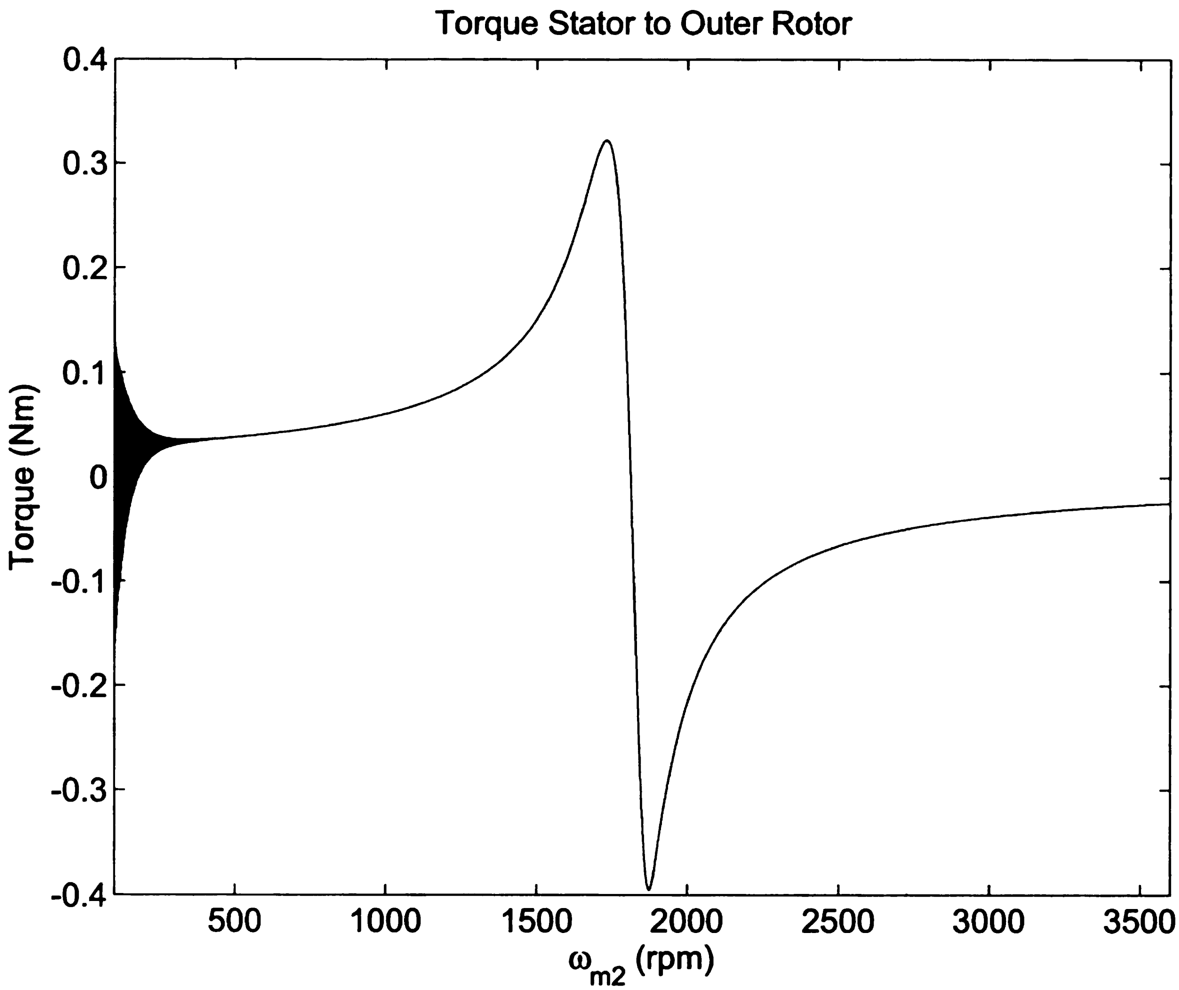

Figure 7.15. Torque between the stator and outer rotor when the inner rotor is an open circuit.

7.8.2 Results

The torque speed curve for the stator is presented in Figure 7.15. During startup, the machine is unstable and then gains stability throughout the remainder of the curve. After the synchronous speed of 1800 rpm, the machine stops acting as a motor and starts acting as a generator.

7.9 Test 9 - Inner Rotor Torque Speed Curve

For this test, the goal is to create the torque speed curve for the inner rotor when the stator is an open circuit. Again, the purpose of this test is to obtain information from the model.

7.9.1 Setup

The voltage of the inner rotor will be set to 120V, $V_s = 120V$. The stator and outer rotor applied voltages will be set to zero, $V_{ir} = V_{or} = 0$. As was the case in the last test, the supply and slip frequencies will be modified directly. The inner rotor frequency will be held constant at synchronous speed, $\omega_{ir} = 2\pi 60$ rad/s. The slip frequency will be varied from 100 rpm to 3600 rpm, $\omega_{slip} = \frac{10\pi}{3}$ to $2\pi 60$. For this test, the inner rotor will be held stationary, $\omega_{m1} = 0$. The slip frequency will be applied directly to the outer rotor, $\omega_{or} = \omega_{slip}$. The stator will be made an open circuit by applying a series resistance of 20 kΩ to each of the inner rotor phases.

As was the case with the Test 8, the result of this test will not be a true torque speed curve. The data found during this test is useful to gain basic characteristic information about the EVT.

7.9.2 Results

The torque speed curve for the inner rotor is presented in Figure 7.16. During startup, the machine is unstable and then gains stability throughout the remainder of the curve. After the synchronous speed of 1800 rpm, the machine stops acting as a motor and starts acting as a generator.

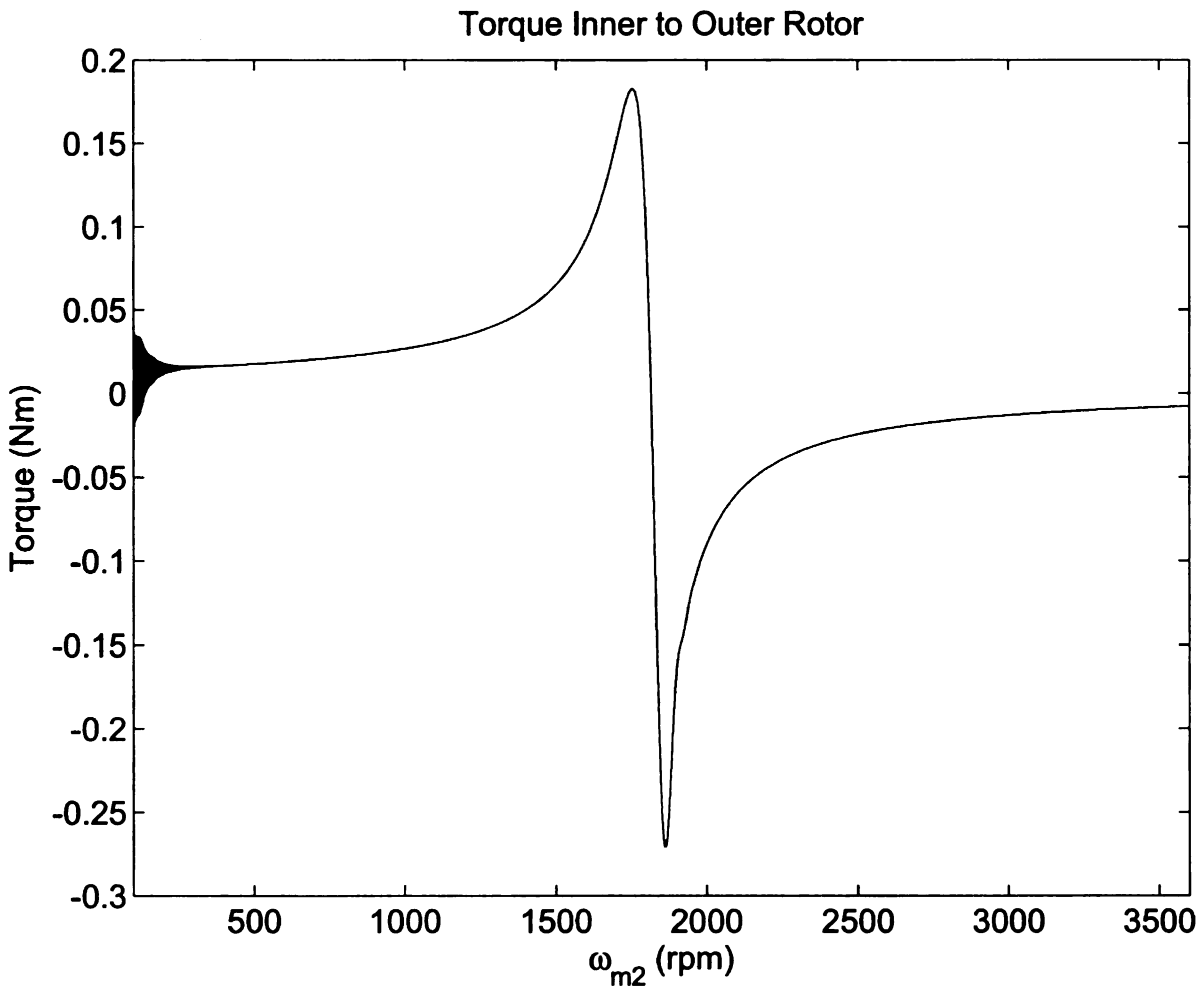

Figure 7.16. Torque between the inner rotor and outer rotor when the stator is an open circuit.

CHAPTER 8

Conclusions

The goal of this work was to create a model for the Electronic Variable Transmission. This objective was met by first determining key motor parameters using finite element analysis. After the methods were developed for determining key parameters, a model was developed using techniques based on the model for a traditional induction machine and adding in special considerations for the physical limitations of the EVT.

This model could be used to determine appropriate applications of an EVT. Different vehicle systems could be investigated to determine the effect of adding an EVT style power transmission device. For example, an EVT style device could be designed using the model developed in this document to replace the current on/off style air conditioning compressor clutches. The entire engine system could be simulated to determine what if any power and subsequent fuel savings could be achieved. There are many areas where an EVT style power transmission device could be applied including modulating a water pump, replacing a mechanical fan drive, replacing a traditional starter and alternator, or any number of power transmission devices.

Once an application of the EVT was determined, a model developed using the method found in this work could be used to determine a proper control algorithm. The control algorithm could be tuned for the specific application. If care is taken in understanding the proper operating points for the given application, the individual motor control for each part of the EVT could then be optimized.

Another application of the model development technique found in this work would be to experiment with different motor types. Rather than using induction machines, a permanent magnet style machine could be investigated. The method developed for finding the model for the EVT could be used by, first finding key parameters using FEA. Then the FEA results could be applied to a pair of traditional permanent magnetic machines to determine the new model. Special considerations for the linkage between the inner rotor and the stator could be taken as they were for the induction machines in this work.

Future work could also include building a prototype machine and testing the results of this work. The model could be verified for steady state operation. The model could then be expanded, taking into consideration transient conditions.

APPENDICES

Appendix A MATLAB Files

A.1 Resistance.m

This file was used to calculate the resistances throughout the EVT.

```
% File: Resistance.m
% Purpose: Calculates the resistances for the stator, inner
%          rotor and outer rotor
% Author: S. Bohan
% Date: 1-17-2007

global Rs Rir Rend Ror

%Coil End Resistances
Rs_end = 0.5575;
Rir_end = 0.5575;

% Resistivities
rho_s  = 0.172e-7; % ohm*m
rho_ir = 0.172e-7; % ohm*m
rho_or = 0.287e-7; % ohm*m

%Stacking Factors
sf_s = 0.8;
sf_ir = 0.8;
sf_or = 1;

% Dimensions
length  = 235e-3;     % meters
area_s  = 72e-6; % meters^2
```

```
area_ir = 87.71e-6;  % meters^2
area_or = 68.94e-6;   % meters^2

% Number of winding turns
N_s  = 44;
N_ir = 44;
N_or = 1;

% Number of slots per phase
s_s  = 4;
s_ir = 3;

% Slot Resistences
Rs_slot  = N_s^2*((rho_s*length)/(sf_s*area_s));
Rir_slot = N_ir^2*((rho_ir*length)/(sf_ir*area_ir));
Ror_bar  = N_or^2*((rho_or*length)/(area_or*sf_or));

% Phase Resistance
Rs  = s_s  * Rs_slot + Rs_end;  % ohm
Rir = s_ir * Rir_slot + Rir_end; % ohm
Ror = Ror_bar;              % ohm

% End Resistance (non calculated value)
Rend = 2.5e-6; % ohm
```

A.2 SMI_SIR.m

This file, along with the "InductanceFromFile.m" file, were used to find the self and mutual inductances associated with the stator and the mutual inductances between the stator and the inner and outer rotors. These files were also used to find the self and mutual inductances associated with the inner rotor and the mutual inductances between the inner rotor and the stator and outer rotor.

```
% File: SMI_SIR.m
% Purpose: Calculates the self and mutual inductances
%          between the stator and  inner rotor
% Author: S. Bohan
% Date: 2-7-2008

Lsa = InductanceFromFile('Flux2d_Data_Sets\SIA_Voltages.txt');
Lsb = InductanceFromFile('Flux2d_Data_Sets\SIB_Voltages.txt');
Lsc = InductanceFromFile('Flux2d_Data_Sets\SIC_Voltages.txt');
Lira = InductanceFromFile('Flux2d_Data_Sets\IRIA_Voltages.txt');
Lirb = InductanceFromFile('Flux2d_Data_Sets\IRIB_Voltages.txt');
Lirc = InductanceFromFile('Flux2d_Data_Sets\IRIC_Voltages.txt');

L_all = [Lsa' Lsb' Lsc' Lira' Lirb' Lirc'];

%Find Ls and Lir
Ls_ = L_all(1:3,1:3);
Lir_ = L_all(4:6,4:6);

% Back out the angles for the mutual inductances between rotor
% and stator (Note: matlab notation mtrix(row,column)
for m = 1:3
    theta_s = (m-1)*(2*pi/3);
    for n = 4:6
        theta_ir = (n-1)*(2*pi/3);
        Lirs_((n-3),m) = L_all(n,m)/cos(theta_s - theta_ir);
        Lsir_(m,(n-3)) = L_all(m,n)/cos(theta_ir - theta_s);
```

```
    end
end
% Find the mutual inductance between the inner rotor and stator
% as an average
Lsir = mean(mean(abs([Lsir_;Lirs_])));

% Find the Stator to Stator mutual inductance
Ls = (Ls_(1,2)+Ls_(1,3)+Ls_(2,1)+Ls_(2,3)+Ls_(3,1)+Ls_(3,2))/3;
%Find the Leakge Inductance
Lls = mean([Ls_(1,1) Ls_(2,2) Ls_(3,3)]) - Ls;

% Find the Inner Rotor to Inner Rotor Mutual Inductance
Lir = (Lir_(1,2)+Lir_(1,3)+Lir_(2,1)+Lir_(2,3)+Lir_(3,1)...
       +Lir_(3,2))/3;
%Find the Leakge Inductance
Llir = mean([Lir_(1,1) Lir_(2,2) Lir_(3,3)]) - Lir;

% Note: End Inductance is a user entered value
Lsend = 2.1e-3;
Lirend = 2.1e-3;

Lsir2B_as = L_all(7:13,1)'.*(1./(sin((((1:7)*pi)/7)-(pi/6))));
Lasor = mean(Lsir2B_as(1:2));

Lsir2B_bs = L_all(7:13,2)'.*(1./(sin((((1:7)*pi)/7)-(5*pi/6))));
Lbsor = mean(Lsir2B_bs(5:7));

Lsir2B_cs = L_all(7:13,3)'.*(1./(sin((((1:7)*pi)/7)-(pi/2))));
Lcsor = mean(Lsir2B_cs(2:5));


% Find the average mutual inductance
Lsor = (Lasor+Lbsor+Lcsor)/3;

Lsir2B_air = L_all(7:13,4)'.*(1./(sin((((1:7)*pi)/7)-(pi/6))));
Lairor = mean(Lsir2B_air(1:2));

Lsir2B_bir = L_all(7:13,5)'.*(1./(sin((((1:7)*pi)/7)-(5*pi/6))));
Lbiror = mean(Lsir2B_bir(5:7));
```

```
Lsir2B_cir = L_all(7:13,6)'.*(1./(sin((((1:7)*pi)/7)-(pi/2))));
Lciror = mean(Lsir2B_cir(2:5));


% Find the average mutual inductance
Liror = (Lairor+Lbiror+Lciror)/3;
```

A.3 InductanceFromFile.m

This file, along with the "SMI_SIR.m" file, were used to find the self and mutual inductances associated with the stator and the mutual inductances between the stator and the inner and outer rotors. The files also find the self and mutual inductances in the inner rotor as well as between the inner rotor and the stator and outer rotor.

```
% File: InductanceFromFile.m
% Purpose: Calculates the self and mutual inductances
%          between the stator and  inner rotor for a
%          single sourced coil
% Author: S. Bohan
% Date: 2-7-2008

function L = InductanceFromFile(fileName)
data= textread(fileName, '', 'headerlines', 4);

Time = data(:,1);
Voltages = cat(2, data(:,2), data(:,4), data(:,6),...
               data(:,8), data(:,10), data(:,12));
Current = data(:,14);

VectorPotential = cat(2, data(:,16), data(:,18), data(:,20),...
                         data(:,22), data(:,24), data(:,26),...
                         data(:,28));

%Find the magnitudes of the voltages
V = fft(Voltages(1:90,:),90);
P_v = abs(V) / 45;
V_Mag = P_v(2,:);

%Find the magnitude of the current
I = fft(Current(1:90),90);
P_i = abs(I) / 45;
```

```
I_Mag = P_i(2);

%Find the Inductances
X = (V_Mag./I_Mag)-(4*0.1359);
L = X ./ (2*pi*60);

%Find the magnitudes of the vector potentials
for j = 1:7
    for i = 1:89
        if i ~= 45
            VP(i,j) = VectorPotential(i,j)/sin(i*2*pi/90);
        else
            VP(i,j) = VP(i-1,j);
        end
    end
    VP_Mag(j) = mean(VP(:,j));
end

% Define constants
w = 15.45e-3;
N = 44;

% Calculate the flux in the regions a-k
%(Note: matlab notation mtrix(row, column)
for n = 1:6
   Phi_SIR2B(n) = (VP_Mag(n)-VP_Mag(n+1))*w;
end
Phi_SIR2B(n+1) = (VP_Mag(n+1)+VP_Mag(1))*w;


% Calculate the mutual inductances
for h = 1:7
    Inductance_SIR2B(h) = 44*Phi_SIR2B(h)/I_Mag;
end

L = cat(1, L(:), Inductance_SIR2B(:))';
```

A.4 SMI_OR.m

This code reads in all of the data collected from the FEA data for the outer rotor self and mutual inductances. It then finds the self and mutual inductances associated with the outer rotor.

```
% File: SMI_OR.m
% Purpose: Calculates the self and mutual inductances in the
%          outer rotor
% Author: S. Bohan
% Date: 10-21-2006

% Read in all of the Vector Potential values and populate an
% array
% The measured potentials with current applied to 2 bars
% (1 "coil")
% Rows = Vector Potential
% Column # = bar where positive current was applied
% Column #+1 = bar where negative current was applied
% For Example the value in Row 4 Column 2 is the Vector Potential
% of bar 4 with current applied to bar 2 and the opposite
% current to bar 3

VectorPotential_B2B(:,1) =...
    textread('Flux2d_Data_Sets\RB_12_reduced.txt', '');
VectorPotential_B2B(:,2) =...
    textread('Flux2d_Data_Sets\RB_23_reduced.txt', '');
VectorPotential_B2B(:,3) =...
    textread('Flux2d_Data_Sets\RB_34_reduced.txt', '');
VectorPotential_B2B(:,4) =...
    textread('Flux2d_Data_Sets\RB_45_reduced.txt', '');
VectorPotential_B2B(:,5) =...
    textread('Flux2d_Data_Sets\RB_56_reduced.txt', '');
VectorPotential_B2B(:,6) =...
    textread('Flux2d_Data_Sets\RB_67_reduced.txt', '');
VectorPotential_B2B(:,7) = ...
    textread('Flux2d_Data_Sets\RB_71_reduced.txt', '');
```

```
% Define constants
w = 15.45e-3;
I = 0.1;

% Calculate the flux in the regions a-k
% (Note: matlab notation matrix(row, column)
for m = 1:7
    for n = 1:6
        Phi_B2B(n,m) = (VectorPotential_B2B(n,m) -...
                       VectorPotential_B2B(n+1,m))*w;
    end
    Phi_B2B(n+1,m) = (VectorPotential_B2B(n+1,m)+...
                     VectorPotential_B2B(1,m))*w;
end

% Calculate the inductances
for k = 1:7
    for h = 1:7
        Inductance_B2B(k, h) = Phi_B2B(k,h)/I;
    end
end

offset_or = [ 0   2   4   6  -6  -4  -2;
             -2   0   2   4   6  -6  -4;
             -4  -2   0   2   4   6  -6;
             -6  -4  -2   0   2   4   6;
              6  -6  -4  -2   0   2   4;
              4   6  -6  -4  -2   0   2;
              2   4   6  -6  -4  -2   0;]*pi/7;

% Find the mutual inductance by calculating the offdiagonal
% inductances
for k = 1:7
    for h = 1:7
        M(k,h) = Inductance_B2B(k, h)/cos(offset_or(k,h));
    end
end

Lor = sum(sum(abs(M-diag(diag(M)))))/(7^2-7);
```

```
% Find the leakage inductance by calculating the diagonal
% inductance and subtracting from it the mutual inductance
Llor = mean(diag(M)) - Lor;

%Find the end inductance (Note: User entered value)
Lend = 4e-9; % H
```

A.5 Example Test M-Code - EVT_ODE_Ex1.m

Files of this type, along with files similar to "ODE_EVT1.m", were used to simulate the EVT for the 9 model verification tests. All of the other files would be similar with modifications made as were listed in chapter 7. These two files are examples of the code used to simulate Test 1.

```
% Model Verfication for the EVT model
% File: EVT_ODE_Ex1.m
% Purpose: Simulates expirament 1 of the EVT model verfication
%          Applies voltage to the stator and an open circuit to
%          inner rotor.
% Author: S. Bohan
% Date: 1/19/08

%Clean up the workspace
clear all
% Define constants in case other files have modified them
j = sqrt(-1);

%-------------- Defined Values --------------
global p Rs Rir Ror Lls Llir Llor Lsor Lsir Liror Vs Vir Vor wm2
global wm1 wslip Rend Lend Lor Lir Ls ws wir wor Lsend Lirend


P = 4;                    % Unitless
p = P/2;                  % Unitless

% Get the current path
curr_dir = cd;
% Move up a directory
cd ..
cd ('EVT_PROPERTIES')

% Call other m-files to calculate base resistances and
% inductances
```

```
Resistance;
SMI_SIR;
SMI_OR;

% Reset the path
cd(curr_dir);

Vs = 120;
Vir = 0;
Vor = 0;

wm2 = (1785/60)*2*pi;
wm1 = (0/60)*2*pi;
wslip = (30/60)*2*pi;

ws = p*wm2+wslip;
wir = p*(wm2-wm1)+wslip;
wor = wslip;

offset_s =  [0 2 -2; -2 0 2; 2 -2 0]*pi/3;
offset_ir = [0 2 -2; -2 0 2; 2 -2 0]*pi/3;
offset_or = [ 0   2   4   6  -6  -4  -2;
             -2   0   2   4   6  -6  -4;
             -4  -2   0   2   4   6  -6;
             -6  -4  -2   0   2   4   6;
              6  -6  -4  -2   0   2   4;
              4   6  -6  -4  -2   0   2;
              2   4   6  -6  -4  -2   0;]*pi/7;

offset_sor = offset_s(:,1)*[1 1 1 1 1 1 1]...
           + [1 1 1]' * offset_or(1,:);

offset_iror = offset_ir(:,1)*[1 1 1 1 1 1 1]...
           + [1 1 1]' * offset_or(1,:);

offset_sir = offset_s(:,1)*[1 1 1]...
           + [1 1 1]'*offset_ir(1,:);

% Initial realtive positions
% Outer rotor position with respect to stator position
```

```
evt_phi_ir = 0;         % rad
evt_phi_s = 0;
evt_phi_or = 0;

t_step = 1/1000;

%Setup Initial condition vector
T = (0:19999)*t_step;
y0 = [0 0 0 0 0 0 0 0 0 0 0 0 0 evt_phi_s evt_phi_ir...
      evt_phi_or (evt_phi_s-evt_phi_ir)...
      (evt_phi_s-evt_phi_or) (evt_phi_ir-evt_phi_or)];

[T, Y] = ode45(@ODE_EVT1, T, y0);
is = Y(:,1:3);
iir = Y(:,4:6);
ior = Y(:,7:13);
phi_s = Y(:,14);
phi_ir = Y(:,15);
phi_or = Y(:,16);
theta_sir = Y(:,17);
theta_sor = Y(:,18);
theta_iror = Y(:,19);

Vs_ = [sqrt(2)*Vs*sin(Y(:,14)+offset_s(1,1))...
                sqrt(2)*Vs*sin(Y(:,14)+offset_s(2,1))...
                sqrt(2)*Vs*sin(Y(:,14)+offset_s(3,1))];
Vir_ = [sqrt(2)*Vir*sin(Y(:,15)+offset_s(1,1))...
                sqrt(2)*Vir*sin(Y(:,15)+offset_s(2,1))...
                sqrt(2)*Vir*sin(Y(:,15)+offset_s(3,1))];

Trs=-p*Lsir*((is(:,1).*(iir(:,1)-0.5*iir(:,2)-0.5*iir(:,3))...
            +is(:,2).*(iir(:,2)-0.5*iir(:,1)-0.5*iir(:,3))...
            +is(:,3).*(iir(:,3)-0.5*iir(:,2)...
            -0.5*iir(:,1))).*sin(theta_sir)+...
            (sqrt(3)/2)*(is(:,1).*(iir(:,2)-iir(:,3))...
                  +is(:,2).*(iir(:,3)-iir(:,1))...
                  +is(:,3).*(iir(:,1)-iir(:,2)))...
                  .*cos(theta_sir));
```

```
Tml =-p*Liror*((iir(:,1).*(cos(offset_iror(1,1))*ior(:,1)...
                          +cos(offset_iror(1,2))*ior(:,2)...
                          +cos(offset_iror(1,3))*ior(:,3)...
                          +cos(offset_iror(1,4))*ior(:,4)...
                          +cos(offset_iror(1,5))*ior(:,5)...
                          +cos(offset_iror(1,6))*ior(:,6)...
                          +cos(offset_iror(1,7))*ior(:,7))...
               +iir(:,2).*(cos(offset_iror(2,1))*ior(:,1)...
                          +cos(offset_iror(2,2))*ior(:,2)...
                          +cos(offset_iror(2,3))*ior(:,3)...
                          +cos(offset_iror(2,4))*ior(:,4)...
                          +cos(offset_iror(2,5))*ior(:,5)...
                          +cos(offset_iror(2,6))*ior(:,6)...
                          +cos(offset_iror(2,7))*ior(:,7))...
               +iir(:,3).*(cos(offset_iror(3,1))*ior(:,1)...
                          +cos(offset_iror(3,2))*ior(:,2)...
                          +cos(offset_iror(3,3))*ior(:,3)...
                          +cos(offset_iror(3,4))*ior(:,4)...
                          +cos(offset_iror(3,5))*ior(:,5)...
                          +cos(offset_iror(3,6))*ior(:,6)...
                          +cos(offset_iror(3,7))*ior(:,7)))...
                          .*sin(theta_iror)+...
              (iir(:,1).*(sin(offset_iror(1,1))*ior(:,1)...
                          +sin(offset_iror(1,2))*ior(:,2)...
                          +sin(offset_iror(1,3))*ior(:,3)...
                          +sin(offset_iror(1,4))*ior(:,4)...
                          +sin(offset_iror(1,5))*ior(:,5)...
                          +sin(offset_iror(1,6))*ior(:,6)...
                          +sin(offset_iror(1,7))*ior(:,7))...
               +iir(:,2).*(sin(offset_iror(2,1))*ior(:,1)...
                          +sin(offset_iror(2,2))*ior(:,2)...
                          +sin(offset_iror(2,3))*ior(:,3)...
                          +sin(offset_iror(2,4))*ior(:,4)...
                          +sin(offset_iror(2,5))*ior(:,5)...
                          +sin(offset_iror(2,6))*ior(:,6)...
                          +sin(offset_iror(2,7))*ior(:,7))...
               +iir(:,3).*(sin(offset_iror(3,1))*ior(:,1)...
                          +sin(offset_iror(3,2))*ior(:,2)...
                          +sin(offset_iror(3,3))*ior(:,3)...
                          +sin(offset_iror(3,4))*ior(:,4)...
```

```
                          +sin(offset_iror(3,5))*ior(:,5)...
                          +sin(offset_iror(3,6))*ior(:,6)...
                          +sin(offset_iror(3,7))*ior(:,7)))...
                          .*cos(theta_iror));
Tm2 =-p*Lsor*((is(:,1).*(cos(offset_iror(1,1))*ior(:,1)...
                          +cos(offset_iror(1,2))*ior(:,2)...
                          +cos(offset_iror(1,3))*ior(:,3)...
                          +cos(offset_iror(1,4))*ior(:,4)...
                          +cos(offset_iror(1,5))*ior(:,5)...
                          +cos(offset_iror(1,6))*ior(:,6)...
                          +cos(offset_iror(1,7))*ior(:,7))...
              +is(:,2).*(cos(offset_iror(2,1))*ior(:,1)...
                          +cos(offset_iror(2,2))*ior(:,2)...
                          +cos(offset_iror(2,3))*ior(:,3)...
                          +cos(offset_iror(2,4))*ior(:,4)...
                          +cos(offset_iror(2,5))*ior(:,5)...
                          +cos(offset_iror(2,6))*ior(:,6)...
                          +cos(offset_iror(2,7))*ior(:,7))...
              +is(:,3).*(cos(offset_iror(3,1))*ior(:,1)...
                          +cos(offset_iror(3,2))*ior(:,2)...
                          +cos(offset_iror(3,3))*ior(:,3)...
                          +cos(offset_iror(3,4))*ior(:,4)...
                          +cos(offset_iror(3,5))*ior(:,5)...
                          +cos(offset_iror(3,6))*ior(:,6)...
                          +cos(offset_iror(3,7))*ior(:,7)))...
                          .*sin(theta_sor)+...
              (is(:,1).*(sin(offset_iror(1,1))*ior(:,1)...
                          +sin(offset_iror(1,2))*ior(:,2)...
                          +sin(offset_iror(1,3))*ior(:,3)...
                          +sin(offset_iror(1,4))*ior(:,4)...
                          +sin(offset_iror(1,5))*ior(:,5)...
                          +sin(offset_iror(1,6))*ior(:,6)...
                          +sin(offset_iror(1,7))*ior(:,7))...
              +is(:,2).*(sin(offset_iror(2,1))*ior(:,1)...
                          +sin(offset_iror(2,2))*ior(:,2)...
                          +sin(offset_iror(2,3))*ior(:,3)...
                          +sin(offset_iror(2,4))*ior(:,4)...
                          +sin(offset_iror(2,5))*ior(:,5)...
                          +sin(offset_iror(2,6))*ior(:,6)...
                          +sin(offset_iror(2,7))*ior(:,7))...
```

```
                    +is(:,3).*(sin(offset_iror(3,1))*ior(:,1)...
                               +sin(offset_iror(3,2))*ior(:,2)...
                               +sin(offset_iror(3,3))*ior(:,3)...
                               +sin(offset_iror(3,4))*ior(:,4)...
                               +sin(offset_iror(3,5))*ior(:,5)...
                               +sin(offset_iror(3,6))*ior(:,6)...
                               +sin(offset_iror(3,7))*ior(:,7)))...
                               .*cos(theta_sor));

% Create Time Based Figure
figure1 = figure;

% Create Plot 1
axes1 = axes('Position',[0.13 0.7093 0.775 0.2157],...
             'Parent',figure1);
box('on');
hold('all');
xlabel('Time (sec)');
ylabel('Current (A)');
title('Stator Current - Phase A & B');
xlim([19.8 20]);
plot1 = plot(T,is(:,1), 'Parent', axes1);
plot2 = plot(T,is(:,2), 'Parent', axes1);
set(plot1,'Color',[0 0 0]);
set(plot2, 'Color',[0.3137 0.3137 0.3137], 'LineStyle','--');
% Create legend
legend1 = legend(axes1,{'I_{as}','I_{bs}'});

% Create Plot 2
axes2 = axes('Position',[0.13 0.4096 0.775 0.2157],...
             'Parent',figure1);
box('on');
hold('all');
xlabel('Time (sec)');
ylabel('Current (A)');
title('Outer Rotor Current - Phase A & B');
xlim([15 20]);
plot3 = plot(T,ior(:,1), 'Parent', axes2);
plot4 = plot(T,ior(:,2), 'Parent', axes2);
set(plot3,'Color',[0 0 0]);
```

```
set(plot4, 'Color',[0.3137 0.3137 0.3137], 'LineStyle','--');
% Create legend
legend2 = legend(axes2,{'I_{aor}','I_{bor}'});

axes3 = axes('Position',[0.13 0.11 0.775 0.2157],...
             'Parent',figure1);
box('on');
box('on');
hold('all');
xlabel('Time (sec)');
ylabel('Current (A)');
title('Inner Rotor Current - Phase A & B');
xlim([19.8 20]);
plot5 = plot(T,iir(:,1), 'Parent', axes3);
plot6 = plot(T,iir(:,2), 'Parent', axes3);
set(plot5,'Color',[0 0 0]);
set(plot6, 'Color',[0.3137 0.3137 0.3137], 'LineStyle','--');
% Create legend
legend3 = legend(axes3,{'I_{air}','I_{bir}'});

figure3 = figure;

% Create Plot 4
axes4 = axes('Position',[0.13 0.7093 0.775 0.2157],...
             'Parent',figure3);
box('on');
hold('all');
title('Torque Inner Airgap');
xlabel('Time (sec)');
ylabel('Torque (Nm)');
xlim([0 5]);
plot7 = plot(T,Tm1(:,1), 'Parent', axes4);

% Create Plot 5
axes5 = axes('Position',[0.13 0.4096 0.775 0.2157],...
             'Parent',figure3);
box('on');
hold('all');
xlabel('Time (sec)');
ylabel('Torque (Nm)');
```

```
title('Torque Stator and Inner Rotor');
xlim([0 5]);
plot8 = plot(T,Trs(:,1), 'Parent', axes5);

% Create Plot 6
axes6 = axes('Position',[0.13 0.11 0.775 0.2157],...
            'Parent',figure3);
box('on');
hold('all');
title('Torque Outer Airgap');
xlabel('Time (sec)');
ylabel('Torque (Nm)');
xlim([0 5]);
plot9 = plot(T,Tm2(:,1), 'Parent', axes6);

%Create Frequency Based figure
figure2 = figure;

f = 1000*(0:200)/1000;

% Create Plot 7
axes7 = axes('Position',[0.13 0.7106 0.3347 0.211],...
            'Parent',figure2);
box('on');
hold('all');
title('Frequency content of ias')
xlabel('frequency (Hz)')
%Find major frequency components
F = fft(is(:,1),1000);
Pff = F.* conj(F)/1000;
plot10 = plot(f,Pff(1:201), 'Parent', axes7);

% Create Plot 8
axes8 = axes('Position',[0.5703 0.7106 0.3347 0.211],...
            'Parent',figure2);
box('on');
hold('all');
title('Frequency content of iaor')
xlabel('frequency (Hz)')
%Find major frequency components
```

```
F = fft(ior(:,1),1000);
Pff = F.* conj(F)/1000;
plot11 = plot(f,Pff(1:201), 'Parent', axes8);

% Create Plot 9
axes9 = axes('Position',[0.13 0.4109 0.3347 0.211],...
             'Parent',figure2);
box('on');
hold('all');
title('Frequency content of iair');
xlabel('frequency (Hz)')
%Find major frequency components
F = fft(iir(:,1),1000);
Pff = F.* conj(F)/1000;
plot12 = plot(f,Pff(1:201), 'Parent', axes9);

% Create Plot 10
axes10 = axes('Position',[0.5703 0.4109 0.3347 0.211],...
              'Parent',figure2);
box('on');
hold('all');
title('Frequency content of Vas')
xlabel('frequency (Hz)')
%Find major frequency components
F = fft(Vs_(:,1),1000);
Pff = F.* conj(F)/1000;
plot13 = plot(f,Pff(1:201), 'Parent', axes10);

% Create Plot 12
axes12 = axes('Position',[0.5703 0.11 0.3255 0.2157],...
              'Parent',figure2);
box('on');
hold('all');
title('Frequency content of Vair')
xlabel('frequency (Hz)')
%Find major frequency components
F = fft(Vir_(:,1),1000);
Pff = F.* conj(F)/1000;
plot15 = plot(f,Pff(1:201), 'Parent', axes12);
```

A.6 Example Test M-Code - ODE_EVT1.m

Files of this type, along with files similar to "EVT_ODE_Ex1.m", were used to simulate the EVT for the 9 model verification tests. All of the other files would be similar with modifications made as were listed in chapter 7. These two files are examples of the code used to simulate Test 1.

```
function dy = ODE_EVT1(t,y)
dy=zeros(19,1);

global p Rs Rir Ror Lls Llir Llor Lsor Lsir Liror Vs Vir Vor wm2
global  wm1 wslip Rend Lend Lor Lir Ls ws wir wor Lsend Lirend

offset_s =  [0 2 -2; -2 0 2; 2 -2 0]*pi/3;
offset_ir = [0 2 -2; -2 0 2; 2 -2 0]*pi/3;
offset_or = [  0   2   4   6  -6  -4  -2;
              -2   0   2   4   6  -6  -4;
              -4  -2   0   2   4   6  -6;
              -6  -4  -2   0   2   4   6;
               6  -6  -4  -2   0   2   4;
               4   6  -6  -4  -2   0   2;
               2   4   6  -6  -4  -2   0;]*pi/7;
offset_sor = offset_s(:,1)*[1 1 1 1 1 1 1]...
           + [1 1 1]' * offset_or(1,:);

offset_iror = offset_ir(:,1)*[1 1 1 1 1 1 1]...
           + [1 1 1]' * offset_or(1,:);

offset_sir = offset_s(:,1)*[1 1 1]...
           + [1 1 1]'*offset_ir(1,:);

Vs_ = sqrt(2)*Vs*sin(y(14)+offset_s(:,1));
Vir_ = sqrt(2)*Vir*sin(y(15)+offset_ir(:,1));
Vor_ = zeros(7, 1);

V_ = [Vs_;Vir_;Vor_];
```

```
% Setup the resitence matrices
Rs_ = Rs * eye(3);
Rir_ = (Rir+20e3)*eye(3);
Ror_p = Ror * eye(7);
Ror_b = circshift(Ror_p,[0,-1]);
Ror_f = circshift(Ror_p,[0,1]);
Rend_ = (2*Rend/7) * eye(7);
Ror_ = 2*Ror_p-Ror_b-Ror_f+Rend_;

Ls_ = Ls * cos(offset_s)+(Lls+Lsend)*eye(3);
Lir_ = Lir * cos(offset_ir)+(Llir+Lirend)*eye(3);
Lend_= ((2*Lend/7)+Llor) * eye(7);
Lor_ = Lend_+Lor*cos(offset_or);

Lsir_ = Lsir .* [cos(y(17)+offset_sir)];
Lirs_ = Lsir_';

dLsir_ = -Lsir*(cos(offset_sir)*sin(y(17))...
         +sin(offset_sir)*cos(y(17)));
dLirs_ = dLsir_';

Lsor_ = Lsor .* [cos(y(18)+offset_sor)];
Lors_ = Lsor_';

dLsor_ = -Lsor*(cos(offset_sor)*sin(y(18))...
         +sin(offset_sor)*cos(y(18)));
dLors_ = dLsor_';

Liror_ = Liror .* [cos(y(19)+offset_iror)];
Lorir_ = Liror_';

dLiror_ = -Liror*(cos(offset_iror)*sin(y(19))...
          +sin(offset_iror)*cos(y(19)));
dLorir_ = dLiror_';

A = [Rs_ dLsir_*p*wm1 dLsor_*p*wm2;...
    dLirs_*p*wm1 Rir_ dLiror_*p*(wm2-wm1);...
    dLors_*p*wm2 dLorir_*p*(wm2-wm1) Ror_];
```

```
B = [Ls_ Lsir_ Lsor_;...
     Lirs_ Lir_ Liror_;...
     Lors_ Lorir_ Lor_];

dy(1:13)=inv(B)*(V_ - A*y(1:13));
dy(14) = ws;                              %dphi_s
dy(15) = wir;                             %dphi_ir
dy(16) = wor;                             %dphi_or
dy(17) = p*wm1;
dy(18) = p*wm2;
dy(19) = p*(wm2-wm1);
```

Appendix B Geometry

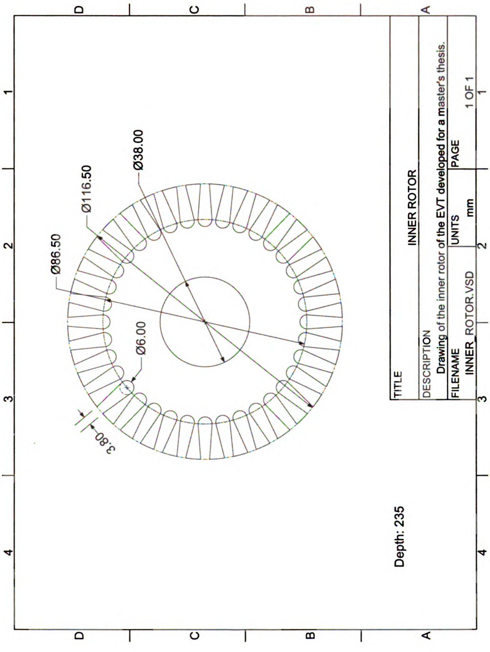

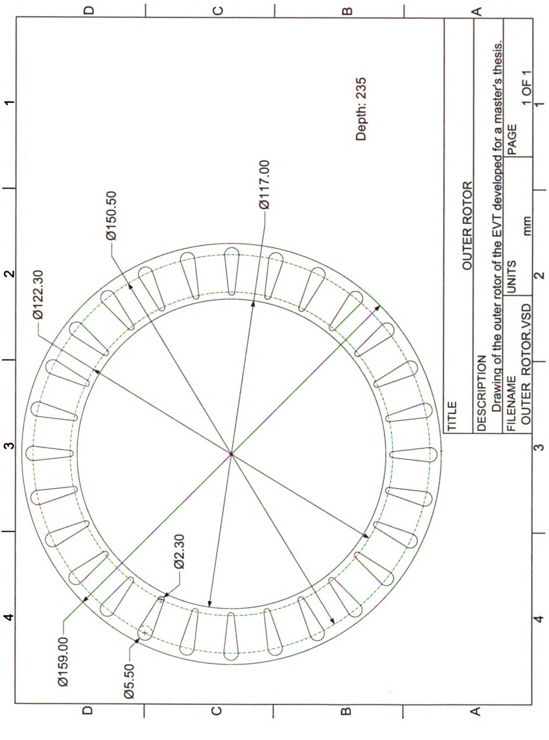
Ø122.30
Ø150.50
Ø117.00
Depth: 235
Ø2.30
Ø159.00
Ø5.50
TITLE
OUTER ROTOR
DESCRIPTION
Drawing of the outer rotor of the EVT developed for a master's thesis.
FILENAME
OUTER ROTOR.VSD
UNITS
mm
PAGE
1 OF 1

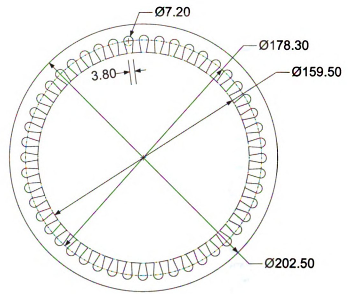

Depth: 235

TITLE STATOR		
DESCRIPTION Drawing of the stator of the EVT developed for a master's thesis.		
FILENAME STATOR.VSD	UNITS mm	PAGE 1 OF 1

BIBLIOGRAPHY

BIBLIOGRAPHY

[1] T. Backstrom, C. Sadarangani and S. Ostlund. Integrated Energy Transducer for Hybrid Electric Vehicles. *Eighth International Conference on Electrical Machines and Drives* pages 239–243, September 1997.

[2] C.C. Chan. The State of the Art of Electric, Hybrid, and Fuel Cell Vehicles. *Proceedings of the IEEE.* pages 704–718, April 2007.

[3] D.K. Cheng. *Field and Wave Electromagnetics.* Addison-Wesley Publishing Company, 1992.

[4] M.J. Hoeijmakers and J.A. Ferreira. The Electric Variable Transmission. *IEEE Industry Applications Conference*, pages 2770–2777, October 2004.

[5] P.C. Krause, O. Wasynczuk, and S.D. Sudhoff. *Analysis of Electric Machinery and Drive Systems.* IEEE Press, 2002.

[6] J.M. Miller. Hybrid Electric Vehicle Propulsion System Architectures of the e-CVT Type. *IEEE Transactions on Power Electronics*, pages 756–767, May 2006.

[7] A.R. Muñoz and T.A. Lipo. Complex Vector Model of the Squirrel-Cage Induction Machine Including Instantaneous Rotor Bar Currents. *IEEE Transactions on Industry Applications*, pages 1332–1340, November/December 1999.

[8] E. Nordlund and C. Sadarangani. Four-quadrent Energy Transducer for Hybrid Electric Vehicles. *Record of the Industry Applications Conference, 2002. 37th IAS Annual Meeting. Conference*, pages 390–397, 2002.